

**September 4, 2021**

**ICE, CLOUD, AND LAND ELEVATION SATELLITE-2  
(ICESat-2)**

**Algorithm Theoretical Basis Document  
(ATBD)**

**for  
ATL19**

**Gridded Dynamic Ocean Topography**

**Prepared By:**

**ICESat-2 Science Definition Team Ocean Working Group**

**Contributors**

**James Morison  
David Hancock  
Suzanne Dickinson  
John Robbins  
Leeanne Roberts**

**/Code:**



---

**Goddard Space Flight Center  
Greenbelt, Maryland**

## **Abstract**

This document describes the theoretical basis of the ocean processing algorithms and the products that are produced by the ICESat-2 mission. It includes descriptions of the parameters that are provided in each product as well as ancillary geophysical parameters, which are used in the derivation of these ICESat-2 products.

*ICESat-2 Algorithm Theoretical Basis Document for Gridded Dynamic Ocean Topography*

*Release 001*

## **CM Foreword**

This document is an Ice, Cloud, and Land Elevation Satellite-2 (ICESat-2) Project Science Office controlled document. Changes to this document require prior approval of the Science Development Team ATBD Lead or designee. Proposed changes shall be submitted in the ICESat-II Management Information System (MIS) via a Signature Controlled Request (SCoRe), along with supportive material justifying the proposed change.

In this document, a requirement is identified by “shall,” a good practice by “should,” permission by “may” or “can,” expectation by “will,” and descriptive material by “is.”

Questions or comments concerning this document should be addressed to:

ICESat-2 Project Science Office  
Mail Stop 615  
Goddard Space Flight Center  
Greenbelt, Maryland 20771

*ICESat-2 Algorithm Theoretical Basis Document for Gridded Dynamic Ocean Topography*  
**Release 001**

## **Preface**

This document is the Algorithm Theoretical Basis Document for the processing open ocean data to be implemented at the ICESat-2 Science Investigator-led Processing System (SIPS). The SIPS supports the ATLAS (Advance Topographic Laser Altimeter System) instrument on the ICESat-2 Spacecraft and encompasses the ATLAS Science Algorithm Software (ASAS) and the Scheduling and Data Management System (SDMS). The science algorithm software will produce Level 0 through Level 4 standard data products as well as the associated product quality assessments and metadata information.

The ICESat-2 Science Development Team, in support of the ICESat-2 Project Science Office (PSO), assumes responsibility for this document and updates it, as required, as algorithms are refined or to meet the needs of the ICESat-2 SIPS. Reviews of this document are performed when appropriate and as needed updates to this document are made. Changes to this document will be made by complete revision.

Changes to this document require prior approval of the Change Authority listed on the signature page. Proposed changes shall be submitted to the ICESat-2 PSO, along with supportive material justifying the proposed change.

Questions or comments concerning this document should be addressed to:

Tom Neumann, ICESat-2 Project Scientist  
Mail Stop 615  
Goddard Space Flight Center  
Greenbelt, Maryland 20771

*ICESat-2 Algorithm Theoretical Basis Document for Gridded Dynamic Ocean Topography*  
**Release 001**

## **Review/Approval Page**

**Prepared by:**

*Jamie Morison  
Senior Principal Oceanographer  
Affiliate Professor, Oceanography  
University of Washington, Applied Physics  
Laboratory*

**Reviewed by:**

*Steve Nerem  
Professor  
Associate Director of Colorado Center for  
Astrodynamics Research  
University of Colorado, Boulder*

*Laurie Padman  
Senior Scientist  
President  
Earth & Space Research*

**Approved by:**

*Tom Neumann  
Project Scientist, ICESat-2  
NASA Goddard Spaceflight Center, Code  
615*

**\*\*\* Signatures are available on-line at: [https:// /icesatiimis.gsfc.nasa.gov](https://icesatiimis.gsfc.nasa.gov) \*\*\***



### Change History Log

Revision Level	Description of Change	SCoRe No.	Date Approved
	<p>Initial Release                      (11/9/2020 – Section 5.6.3.2.1 regarding equation 48 description, changed “cross product” to “product sum”)                      The last ATL12 ATBD with a complete ATL19 description is ICESat2_JMdraft_Ocean_atbd_12012020_SD dated Jan. 4, 2021. Changes to ATL19 prior to 11/09/2020 are included in that ATL12 ATBD dated 12/30/2020, ICESat2_JMdraft_Ocean_atbd_12302020_CX.                      Changes to ATL19 ATBD from 12/3/2020 through 12/30/2020 were not tracked or logged and this ATBD originating as Morison’s:  <b>ATL12 ATBD ICESat2_JMdraft_Ocean_atbd_12302020_CX</b> should be considered the original ATL19 ATBD,</p> <p>02/04/2021 Globally corrected <b>grid_lon</b> and <b>grid_lat</b> to <b>lon_avg</b> and <b>lat_avg</b></p> <p>02/04/2021 Corrected the anomaly equations at the end of the first paragraph of Appendix B by multiplying by (1/N)</p> <p>02/22/2021 Finish global change of <b>dof_grid</b> to <b>dof</b></p> <p>02/22/2021 Section 3.2.4.2 correct <b>dot_sigma_dfw_albm</b> to <b>dot_sigma_dfwalbm</b></p> <p>02/22/2021 global change of <b>dot_dfwallbeam</b> to <b>dot_dfwalbm</b></p> <p>02/22/2021 global change of <b>dot_dfw_uncertain</b> to <b>dot_dfw_uncrtn</b></p> <p>02/22/2021 Section 3.2.3.1.1 added computation of uncertainty in simple averages of DOT:                      “To compute the uncertainty, <b>dot_avg_uncrtn</b>, in gridded DOT, <b>dot_avg</b>, divide <b>dot_sigma_avg</b> by the square root of <b>dof</b> to establish the uncertainty in the degree-of-freedom weighted DOT.”                      Also added <b>dot_avg_uncrtn</b> to Table 2</p> <p>02/25/2021 In Table 2 corrected description of <b>dot_avgcntr</b> to</p>		

	<p>“Simple average of dynamic ocean topography interpolated center of grid cell”</p> <p>03/01/2021 In equation 49 corrected the equation for C to <math>c = dot\_avg - (a * lon\_avg + b * lat\_avg)</math></p> <p>04/14/2021 to 4/26/2021 – Numerous small corrections to make variable names consistent throughout</p> <p>04/21/2021 – Section 3.2 Reordered and expanded to:</p> <p>3.2 Gridding DOT and SSH for ATL19 <b>Error! Bookmark not defined.</b></p> <p>3.2.1 The Grids <b>Error! Bookmark not defined.</b></p> <p>3.2.2 Temporal Averaging <b>Error! Bookmark not defined.</b></p> <p>3.2.3 Input to Gridding <b>Error! Bookmark not defined.</b></p> <p>3.2.4 Gridding <b>Error! Bookmark not defined.</b></p> <p>3.2.5 Gridding Output <b>Error! Bookmark not defined.</b></p> <p>and</p> <p>Expand Introduction to include possible ice parameters and optimal interpolation considerations:</p> <p>1.0 INTRODUCTION and Background <b>Error! Bookmark not defined.</b></p> <p>1.1 Background: ATL03 and ATL12 <b>Error! Bookmark not defined.</b></p> <p>1.2 ATL19 Gridded Product <b>Error! Bookmark not defined.</b></p> <p>1.2.1 ATL19 Grids <b>Error! Bookmark not defined.</b></p> <p>1.2.2 The Basic Product <b>Error! Bookmark not defined.</b></p> <p>1.2.3 The running 3-month average <b>Error! Bookmark not defined.</b></p> <p>1.2.4 Merging with ATL10 to produce global DOT <b>Error! Bookmark not defined.</b></p> <p>1.2.5 Optimal interpolation of DOT</p> <p>04/23/2021 Table 2 – Added “_albm” variables</p> <p>04/25/2021 Added Appendix E: Optimal Interpolation of ICESat-2 Dynamic Ocean Topography</p> <p>4/29/2021 Numerous edits for clarity in response to David</p>		
--	---	--	--

	<p>Hancock's comments</p> <p>04/30/2021 – Added Figures 2-6 and related discussions          - Changed Table 2 to Table 3          - Added a new Table 2 listing inter-beam biases</p> <p>6/23/2021 Section 3.2.3.1 Pre-grid filtering was changed to a single pass over ATL12 ocean segments rejecting any ocean segment with average DOT departing from the 10-degree latitude, all-ATL12 average DOT by more than three times the all-ATL12 standard deviation of DOT.</p> <p>9/3/2021 Completed numerous edits suggested by reviewers Laurie Padman and Steve Nerem. This included adding ATL12 background and ATL19 rationale in revised introduction. The noteworthy conceptual addition not mentioned by reviewers was clarifying that the higher moments and uncertainty that are gridded represent only the sea state induced variances and that determining ocean segment-to-segment variability should be addressed with TBD methods.</p> <p>9/4/2021 Added <i>meanoffit2</i> and <i>ds_y_bincenters</i> to Table 1 Inputs from ATL12 and added <i>dot_hist</i>, <i>dot_hist_albm</i>, and <i>ds_y_bincenters</i> to Table 3 Outputs</p> <p>9/4/2021 Changed <i>dot_hist_grid</i> to <i>dot_hist</i> throughout and changed description of calculation of <i>dot_hist</i> to:          “To compute the bin aggregate probability density function (PDF), <i>dot_hist</i>, of DOT, we first must convert each <i>Y</i> PDF from ATL12 to a PDF of DOT by adding <i>meanoffit2</i> to the x-axis of <i>Y</i>, <i>ds_y_bincenters</i> and then interpolating the result to an intermediate PDF, <i>Yintermediate</i>, evaluated at the original <i>ds_y_bincenters</i>. (Note: In ATL19 Release 1, <i>meanoffit2</i> was inadvertently not added so the aggregate histograms only reflect the aggregate wave environment with mean near zero). The aggregate probability PDF, <i>dot_hist</i>, of DOT will equal the sum <i>Yintermediate x n_photons</i> in each histogram bin of all <i>Yintermediate</i> divided by the total, <i>n_photons_gridttl</i>, of all <i>n_photons</i>.”</p>		
--	---	--	--

*ICESat-2 Algorithm Theoretical Basis Document for Gridded Dynamic Ocean Topography*  
**Release 001**



**Table of Contents**

Abstract..... 2-i

CM Foreword ..... ii

Preface ..... iv

Review/Approval Page ..... vi

Change History Log ..... vii

List of TBDs/TBRs ..... xi

List of Figures ..... xiii

List of Tables ..... xiv

1.0 Introduction and Background ..... 1

    1.1 Background: ATL03 and ATL12..... 1

    1.2 ATL19 Gridded Product ..... 3

        1.2.1 ATL19 Grids ..... 3

        1.2.2 The Basic Product..... 3

        1.2.3 All-beam and running 3-month averages ..... 3

        1.2.4 Future Enhancement: Merging with ATL10 to produce global DOT ..... 4

        1.2.5 Future Enhancement: Optimal interpolation of DOT ..... 4

2.0 Gridded Ocean Product (ATL19/ L3B)..... 5

    2.1 Gridded DOT..... 5

        2.1.1 Grid Parameters..... 5

3.0 Algorithm Implementation ..... 7

    3.1 Block Diagram for ATL19 Processing ..... 7

    3.2 Gridding DOT for ATL19 ..... 8

        3.2.1 The Grids ..... 8

        3.2.2 Temporal Averaging..... 9

        3.2.3 Input to Gridding..... 10

        3.2.4 Gridding..... 12

        3.2.5 Gridding Output..... 20

ACRONYMS ..... 26

GLOSSARY ..... 27

APPENDIX A: ICESat-2 Data Products..... 28

APPENDIX B: Fitting a Plane to Spatially Distributed Data..... 33

APPENDIX C: Hierarchy of ATL12 and ATL19 Variables ..... 35

APPENDIX D: All-beam Average Equivalencies ..... 37

APPENDIX E: Optimal Interpolation of ICESat-2 Dynamic Ocean Topography..... 39

## List of Figures

<u>Figure</u>	<u>Page</u>
Figure 1. ICESat-2 spacecraft and beam configuration (left) and footprints flying in the forward direction.....	1
Figure 2. Block diagram for the ATL19 gridding procedure taking ATL12 ocean products as input. m, s, S, and K denote mean, standard deviation, skewness, and kurtosis respectively.....	7
Figure 3. Number of ocean segments found in each grid cell of the $\frac{1}{4}^\circ$ mid-latitude grid in August 2020.....	8
Figure 4. Number of ocean segments in August 2020 in each 25-km grid cell of the north polar stereographic grid (left) and the south polar stereographic grid (right). Color scale is number of ocean segments in a grid cell per month and x and y-axes are in $10^3$ km.....	9
Figure 5. Mid-latitude grid averages of DOT strong beams, Beam 1 (left) and Beam 2 (right), August 2020. Average DOT differences: beam2 – beam1 = 0.61 cm, beam3 – beam1 = 0.55 cm, beam2 – beam3 = -0.08 cm. The blank rectangle in the Central Pacific is the region of ocean–scans not gridded according to the pointing and orbit determination flag.....	14
Figure 6. Mid-latitude DOT gridded by simple “n-segment” all-beam averages (left) and degree-of-freedom weighted (dfw) all-beam averages (right) for August 2020. The ocean scan region in the Central Pacific is not gridded.....	17
Figure 7. Centered grid averages using 9-cells (3x3) to fit to the center of a center cell for 1-month, August 2020, (left) and 3-months, Jul-Aug-Sept. 2020, (right).....	19

## List of Tables

<u>Table</u>	<u>Page</u>
Table 1 Input to ATL19 from ATL12.....	22
Table 2 Inter-beam biases Oct.-Nov. 2020 .....	29
Table 3 Output of ATL19.....	29



*ICESat-2 Algorithm Theoretical Basis Document for Gridded Dynamic Ocean Topography*  
**Release 001**

**1.0 INTRODUCTION AND BACKGROUND**

This ATBD will cover the gridding of dynamic ocean topography and related variables from ICESat-2 ATL12 sea surface height (SSH).

**1.1 Background: ATL03 and ATL12**

The Ice, Cloud and land Elevation Satellite 2 (ICESat-2) is a photon-counting pulsed laser altimeter intended primarily to map the heights of the Earth’s ice and snow-covered and vegetated surfaces. Its Advanced Topographic Laser System (ATLAS) projects 3 pairs of strong and weak beams pulsed at 10 kHz. For each beam, it measures the time of flight of individual photons to the Earth’s surface and back. This range combined with precision pointing and orbit determination is used to measure the height of the surface along ground tracks numbered from left to right (gt1L, gt1R, gt2L, gt2R, gt3L, and gt3R) across the path of ICESat-2 (Fig. 1 right). The 6 beams are arranged in 2 rows of 3 with the weak beams forward when flying in the forward direction. The track assignments of the beams are as shown in Figure 1 (when during half the year ICESat-2 is flying backward the ground tracks remain numbered left to right but the beam assignments flip left to right). With the spacecraft yawed slightly to the left the weak and strong beam tracks of each pair are separated by only 90 m with the tracks of the strong-weak pairs separated 3 km across track. Each pulse of each beam illuminates a patch on the surface about 14-m across, and with the spacecraft moving at 7 km s<sup>-1</sup>, new patches are illuminated every 0.7 m, giving ICESat-2 unparallelled along track spatial resolution. The orbit of ICESat-2 extends to North and South 88° to capture the Polar Regions and repeats every 91 days.

Although ICESat-2 was not intended primarily as an ocean altimeter, its fine resolution and polar reach make it a uniquely exciting ocean instrument. Consequently, the ICESat-2

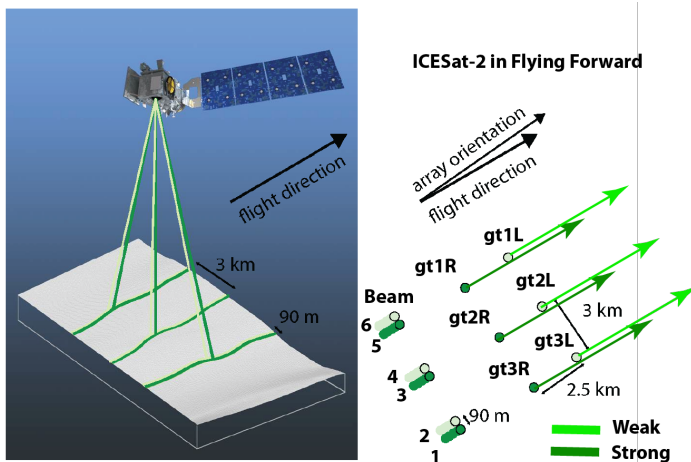


Figure 1. ICESat-2 spacecraft and beam configuration (left) and footprints flying in the forward direction.

ATL12 along track ocean surface height product has been developed (Morison et al., 2019). It draws input data mainly from the ICESat-2 ATL03 Global Geolocated Photon heights product.

The ICESat-2 ATL03 [Neumann et al., 2021a, 2021b] provides the photon reflection height (referred to as photon height) of the ocean surface relative to the WGS84 ellipsoid for the downlinked data of each of the 6 beams. Originally, over the ice-free ocean and away

from land only the strong beam data were downlinked to conserve downlink data volume, and weak beam data was only acquired over the ocean when near land or over sea ice. Beginning in the summer of 2021, this limitation has been relaxed so that strong and weak beam data everywhere is downlinked from the satellite. The raw photon heights are corrected for atmospheric delay and standard geophysical corrections such as solid earth tide of common concern to all the higher-level ICESat-2 products (e.g., land ice, sea ice and vegetation). A statistical approach is used to assign a confidence rating to the likelihood of each photon height being a surface height.

The processing of the ATL03 photon heights to produce the ATL12 ocean surface height [Morison *et al.*, 2019] first involves removing from the photon heights the expected high frequency variations due to tides from the GOT4.8 model and short period atmospheric forcing with a Dynamic Atmospheric Correction (DAC) based on the 6-h AVISO MOG2D. To further reduce the height variability of the raw photon heights, the EGM2008 geoid in the mean tide system is subtracted, so that processing begins with photon heights expressed as dynamic ocean topography (DOT) dealiased for tides and short period atmospheric forcing. The processing system then accumulates histograms of these dealiased and geoid-referenced photon surface heights along each ground track over ocean segments long enough to acquire 8,000 surface-reflected photons or up to a maximum length of 7 km. Minimum ocean segment lengths are usually 3 or 4 km. To better exclude subsurface returns under the crests of waves, surface finding is actually done on the basis of histograms of the photon height anomalies relative to a running 11-point average of the photon heights deemed high confidence surface photons in ATL03. The histogram of these anomalies is then trimmed of noise photons in the high and low tails of the distribution. Once the surface photons are so identified, their actual heights are used in subsequent processing.

To account for the instrumental uncertainty in photon time of flight due mainly to uncertainty in the start time of the photon flights within each laser pulse, the instrument impulse response histogram derived from the downlinked Transmit Echo Pulse (TEP) is deconvolved from the received height histogram to yield a surface histogram.

The ATL12 main outputs are the mean and next three moments of the resulting histogram. The 10-m along-track bin averages of photon heights are computed and used to determine electromagnetic (EM) sea state bias (hereafter referred to as SSB) and wave harmonics projected on to the ground track direction. Uncertainty in the mean surface height is largely due to sampling the wave covered surface and is proportional to significant wave height (SWH) and inversely proportional to the square root of ocean segment length divided by the correlation length scale. For ATL12 Release 4 and beyond, the 10-m along-track averages are used to yield the track-projected wave harmonics, correlation scale, and degrees of freedom.

In addition to data from ICESat-2 ATL03, ATL12 pulls in data from outside sources such ocean depth from GEBCO and in Release 5, ice concentration from NSIDC.

## **1.2 ATL19 Gridded Product**

The ATL19 gridded product is intended to provide users with a realization of the height of the ocean surface mapped over the world ocean in 1-month (and ultimately 3-month) averages. This is in contrast to the ATL12 ocean surface height, which is an along-track record of sea surface height and related variables, each file of which covers only four ICESat-2 orbits representing 6 hours. The primary ATL19 gridded product is dynamic ocean topography (DOT), which is sea surface height relative to the WGS84 ellipsoid minus the height of the EGM 2008, mean-tide geoid [Neumann et al., 2021b] relative to the WGS84 ellipsoid. The ATL12 processing mainly works with DOT to avoid the large variations associated with the geoid, but consistent with prior NASA planning ATL12 outputs ocean segment averages of the SSH and the geoid required to compute ocean segment-averages of DOT. We chose the primary output of ATL19 to be DOT (with the corresponding geoid as an ancillary variable to enable determination of SSH) because the variations in DOT represent familiar circulation patterns and because being much smaller than SSH variations, interbeam biases and error stand out sharply in DOT.

### **1.2.1 ATL19 Grids**

ATL19 uses 3 grids, North and South polar stereographic 25-km grids as well as an overlapping mid-latitude curvilinear  $\frac{1}{4}^\circ$  latitude-longitude grid between  $60^\circ\text{S}$  and  $60^\circ\text{N}$ . The gridding is done individually for each beam on the ocean segments for each beam with average positions inside a grid cell.

### **1.2.2 The Basic Product**

The basic product includes one-month simple averages and averages weighted by the estimated degrees of freedom for each beam ocean segment. Computing the individual beam averages provide a measure of relative biases among the six beams. The simple and degree-of-freedom weighted average grid or latitude-longitude positions of all the beam ocean segments in a grid cell are also output as are the simple and degree-of-freedom weighted averages of other key variables necessary to interpret DOT, such as the geoid and the sea state bias are also provided.

### **1.2.3 All-beam and running 3-month averages**

The present release includes all-beam averages and planar fits over 9 cells to interpolate DOT to grid cell centers. In future releases of ATL19, monthly three-month running averages of the ocean segment DOT will provide more complete filling of grid cells and better interpolation of DOT to the center of the grid cells.

#### **1.2.4 Future Enhancement: Merging with ATL10 to produce global DOT**

DOT as provided by ATL12 in ice covered oceans is biased by the freeboard of the sea ice. In later releases of ATL19 we will account for this in two phases. First, we will work to reconcile any biases between ATL12-derived DOT and DOT from the ATL10 sea ice freeboard product in the low ice concentration regions of the marginal ice zone (MIZ). One possibility that shows initial agreement is to compare ATL10 to the lower of the two ATL12 surface height distributions in the 2-Gaussian mixture representation provided by ATL12 of the DOT distribution. At low ice concentrations we expect this lower component of the Gaussian mixture represents the sea surface and the higher component the ice surface. Once basic biases between ATL10 and ATL12 in the MIZ are resolved, we can subtract the ATL10 freeboard from the apparent ATL12 DOT to yield the true DOT in higher ice concentration regions. Work on this is ongoing with the ICESat-2 Project Office.

#### **1.2.5 Future Enhancement: Optimal interpolation of DOT**

One-month gridded and even three-month gridded ICESat-2 data have unfilled grid cells. We want to provide the ATL19 user with as much information as possible for ICESat-2 to be optimally interpolated over a wide a range of regions and temporal resolutions as well as optimally interpolated global maps of DOT in ATL19. We think the 3-month moving averages that will be part of ATL19 future releases are candidates for the background fields (**B** in Appendix E) underlying DOT anomalies to be interpolated at finer scales. ATL12 and ATL19 are unique in providing degree-of-freedom and uncertainty estimates for ocean segment and gridded DOT, which provide measurement error values for each grid cell observation (**D** in Appendix E). In the future, the key added product in ATL19 will be maps of correlation length scales, possibly in two directions, based on the covariance of regional groups of our  $\frac{1}{4}^\circ$  and polar stereographic gridded ICESat-2 DOT (R in Appendix E).

## **2.0 GRIDDED OCEAN PRODUCT (ATL19/ L3B)**

### **2.1 Gridded DOT**

This product, based on Product ATL12/3A, contains gridded monthly estimates of DOT from all ICESat-2 tracks from the beginning to the end of each month. Below 60°N and above 60°S, the data are mapped on the ¼° curvilinear latitude-longitude grid. In response to reviewer comments, these latitude limits will be increased in the future to 66°N and 66°S to match the region of TOPEX/Poseidon coverage. Above 60°N and below 60°S, the grid data are mapped onto a planimetric grid using the NSIDC Sea Ice Polar Stereographic grids ([https://nsidc.org/data/polar-stereo/ps\\_grids.html](https://nsidc.org/data/polar-stereo/ps_grids.html)) with a grid spacing of 25 km. In the polar oceans the ATL10 sea ice products and ATL21 gridded sea ice products will eventually be reconciled with ATL12 and ATL19 data by methods TBD.

#### **2.1.1 Grid Parameters**

##### **2.1.1.1 DOT**

With only ATL12 needed as input, the primary ATL19 will be grid cell averages of product dynamic ocean topography (DOT), the sea surface departure from the EGM2008 mean-tide geoid. These include simple arithmetic 1-month averages of DOT, degree-of-freedom-weighted averages and multi-cell, least-squares linear interpolations to grid cell centers. Running monthly 3-month averages are planned for the future. In addition to the mean, the product will include standard deviation, skewness, and kurtosis, propagated from 2<sup>nd</sup>, 3<sup>rd</sup>, and 4<sup>th</sup> moments from ATL12 ocean segments included in each grid cell.

The corresponding averages of position, geoid height, SSB, ocean depth and other pertinent parameters from each segment will also be output. The mean SSH can be calculated as the mean DOT plus the weighted average geoid height.

##### **2.1.1.2 Sea surface statistics histogram within grid**

For each month, the aggregate histogram of photon heights expressed as DOT accumulated in the cell for all ocean segments in a grid cell will be output. The mean SSH can be calculated as the mean DOT plus the weighted average geoid height.

##### **2.1.1.3 Wave statistics within grid**

Estimates of SWH and SSB from the *a priori* estimation of sea state bias will also be grid-averaged with appropriate normalization for the number of surface photons in each segment.

*ICESat-2 Algorithm Theoretical Basis Document for Gridded Dynamic Ocean Topography*  
**Release 001**

### 3.0 ALGORITHM IMPLEMENTATION

This section provides a more detailed description of the calculations of the ATL19 gridded products. It is meant to guide the derivation of both the development MATLAB code and the NASA ASAS computer code that will be used to produce ATL19. During development of the ASAS code, its output will be checked against the MATLAB code for selected ATL12 input data.

#### 3.1 Block Diagram for ATL19 Processing

This product, based on Product ATL12/3A, contains gridded monthly estimates of DOT from all ICESat-2 tracks from the beginning to the end of each month. Below 60°N and above 60°S, the data are mapped on the ¼°curvilinear latitude-longitude grid. In response to reviewer comments, these latitude limits will be increased in the future to 66°N and 66°S to match the region of TOPEX/Poseidon coverage. Above 60°N and below 60°S, the grid data are mapped onto a planimetric grid using the NSIDC Sea Ice Polar Stereographic grids ([https://nsidc.org/data/polar-stereo/ps\\_grids.html](https://nsidc.org/data/polar-stereo/ps_grids.html)) with a grid spacing of 25 km.

ATL12 provides the histograms and first four moments of dynamic ocean topography over ocean segments up to 7-km long (DOT can be converted to SSH by adding ocean segment average geoid height, which is also output by ATL12). It also provides the number of photon

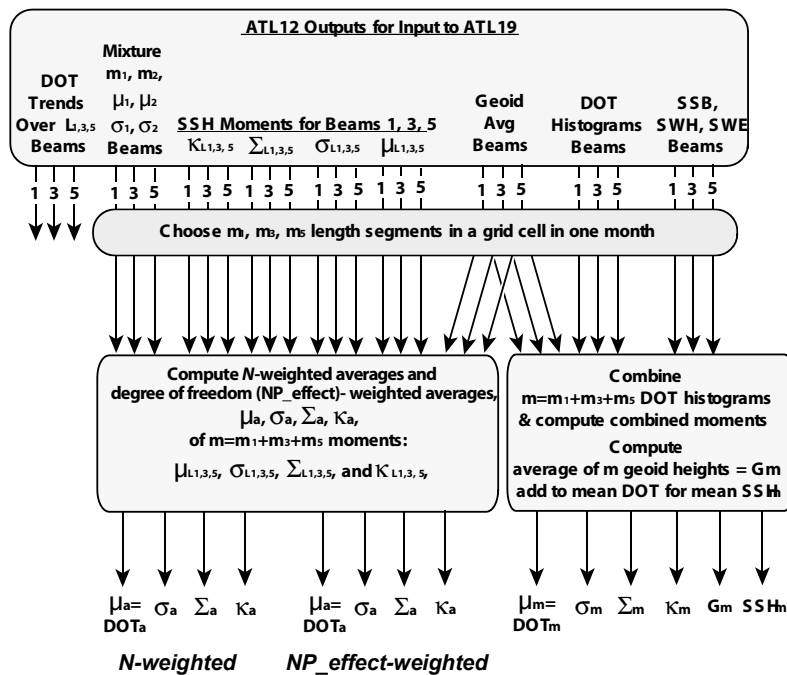


Figure 2. Block diagram for the ATL19 gridding procedure taking ATL12 ocean products as input.  $\mu, \sigma, \Sigma$ , and  $K$  denote mean, standard deviation, skewness, and kurtosis respectively.



heights,  $n\_photons$ , going into the moments and an effective degrees-of-freedom,  $NP\_effect$ , based on the correlation length scale of surface heights. Using these, ATL19 will produce monthly aggregate histograms of surface heights and averages of the ocean segment moments weighted by both  $n\_photons$  and  $NP\_effect$  (Fig. 2).

### 3.2 Gridding DOT for ATL19

The ATL19 product includes gridded monthly estimates of dynamic ocean topography (DOT) taken from ATL12 ocean segment data. Ocean segments range in length roughly from 3 to a maximum 7 km dependent on photon rate. For ATL19 the ocean segment data are averaged in  $\frac{1}{4}^\circ$  latitude-longitude or 25-km polar stereographic grid cells. Data from all six beams are used, both individually and averaged together from the beginning to the end of each month, prior to the summer of 2021 only strong beam data were downlinked and available over most of the ocean.

#### 3.2.1 The Grids

The ICESat-2 data from ATL12 are averaged onto three grids, called mid-latitude, north-polar and south-polar. The ATL19 data file has groups with similar names containing the gridded data from each of those regions. It is important to note that when we do gridding of individual beams (or in ATLAS terminology: spots) it does not imply that the individual ground tracks, gt1l; gt1r; gt2l; gt2r; gt3l; gt3r, from ATL12 are averaged. This is avoided due to the fact that the ground track of a beam changes depending on the flight direction of the spacecraft (Fig. 1) For ATL19, strong beams are kept together over yaw flips. This is so that knowing average DOT differences across grid cells is small, we can use the individual

beam gridded DOT values for calculating the bias between spots/beams.

The mid-latitude group contains ocean segment data mapped onto the curvilinear,  $\frac{1}{4}^\circ$  latitude-longitude grid extending from  $60^\circ$  to  $66^\circ$  (Fig. 3), to be expanded in future releases to  $66^\circ$ S to  $66^\circ$ N. The grid cells are centered on the odd  $\frac{1}{8}^{\text{th}}$  degree, with the latitude and longitude matrices defined in *gridcntr\_lat* and *gridcntr\_lon*, respectively. The matrix size of the gridded variables in the mid-latitude group is [480 x 1440].

As with the ATL20 product, ATL19 uses the North and South NSIDC Sea Ice Polar Stereographic grids (Fig. 4, <https://nsidc.org/data/polar->

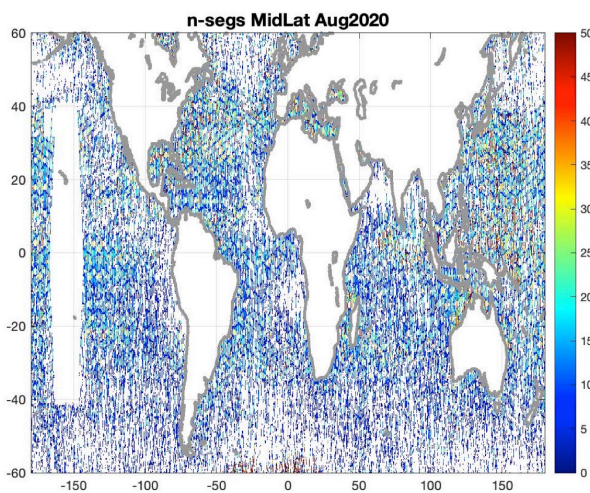


Figure 3. Number of ocean segments found in each grid cell of the  $\frac{1}{4}^\circ$  mid-latitude grid in August 2020.

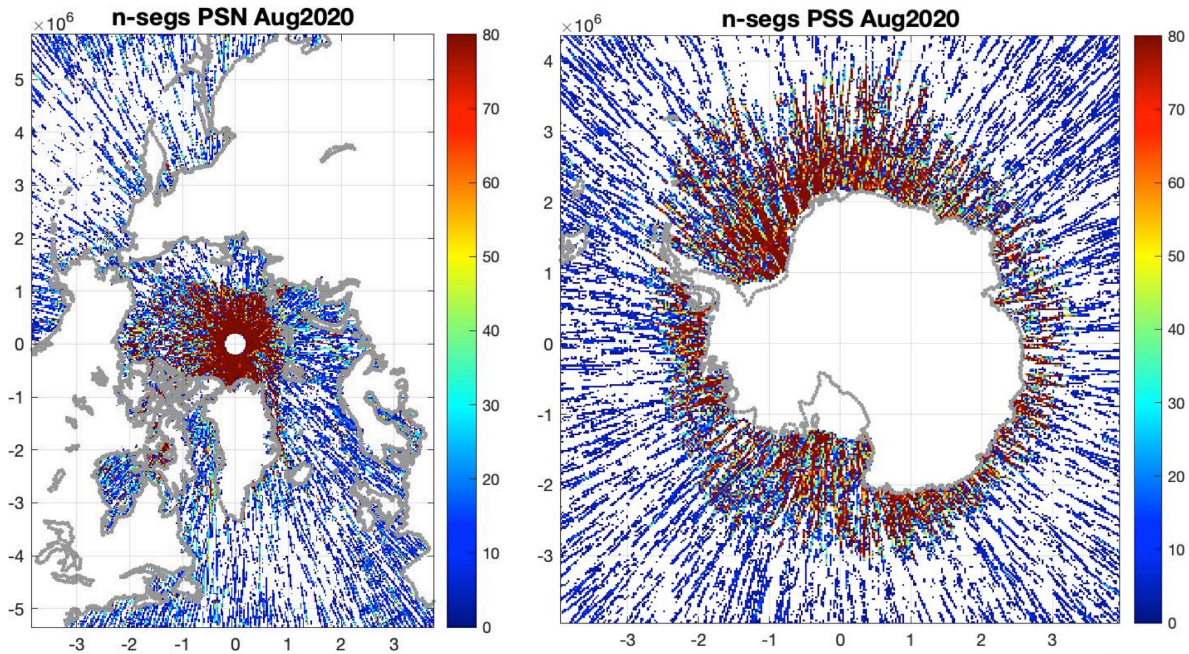


Figure 4. Number of ocean segments in August 2020 in each 25-km grid cell of the north polar stereographic grid (left) and the south polar stereographic grid (right). Color scale is number of ocean segments in a grid cell per month and x and y-axes are in  $10^3$  km.

(<https://epsg.io/3411>) to project data poleward of 60 degrees latitude. Both grids have a grid spacing of 25 km, equivalent to  $\frac{1}{4}$  degree of latitude and are relative to the Hughes 1980 Ellipsoid. The origins of these grids are at the poles and expressed in x and y distances from the poles. The North polar grid (<https://epsg.io/3411>) matrix is of size [448 x 304], with a true distance at 70°N and a central longitude along 45°W-135°E, with y positive along 135°E and x positive along 45°E. The South polar grid (<https://epsg.io/3412>) matrix is of size [332 x 316], with a true distance at 70°S and a central longitude along 180°- 0°E with y positive along 0°E and x positive along 90°E. The ATL19 defined grid variables for the polar regions are *ds\_grid\_x* and *ds\_grid\_y*. The north-polar and south-polar groups also contain *gridcntr\_lat* and *gridcntr\_lon*, similar to the mid-latitude group with latitude and longitude values converted from the x and y values in *ds\_grid\_x*, and *ds\_grid\_y*.

Major portions of each of these grids are not ocean, and the gridded sea surface height values for these grid cells will be set to a default invalid value.

### 3.2.2 Temporal Averaging

ATL19 includes monthly one-month averages and ultimately it will include monthly 3-month moving averages. The monthly 1-month data include aggregate histograms of DOT and averages of the ocean segment moments for data from all beams together and for each beam individually. The monthly gridded averages mid-latitude and polar grids do not produce averages for every grid cell, the sparseness of the averages being most pronounced at low latitudes. At the equator, the ICESat-2 orbits provide only one satellite pass per  $\frac{1}{4}$ ° of longitude over the 91-day repeat cycle.

Consequently, to provide better data coverage and allow a least squares linear interpolation of DOT to grid cell centers, ATL19 will also include a monthly 3-month moving average that includes a least-squares planar fit among 9 (3X3) grid cells to grid cell centers. The goal is to provide data for every grid cell that is not perpetually under a heavy cloud cover.

### **3.2.3 Input to Gridding**

Input to the ATL19 gridding process for each beam (ATLAS spot) includes the first four moments of sea surface height; mean SSH,  $h$ , variance of SSH,  $h\_var$ , skewness of SSH,  $h\_skewness$ , and kurtosis of SSH,  $h\_kurtosis$ , for each ocean segment from ATL12 (the moments in ATL12 are computed on DOT and the geoid is added to the mean to produce  $h$ ). Simple averages and averages weighted by the degrees-of-freedom for each ocean segment are included. The gridded DOT is taken as sea surface height,  $h$ , minus the geoid height,  $geoid\_seg$ .<sup>\*</sup> The gridded DOT variance, skewness, and kurtosis are derived from  $h\_var$ ,  $h\_skewness$ , and  $h\_kurtosis$  respectively. Other geophysical variables gridded from the ATL12 include significant wave height,  $swh$ , sea state bias,  $bin\_ssbias$  and the aggregation of  $y$  histograms. (Note: ATL12  $y$  is the histogram of DOT over an ocean segment minus  $meanoffit2$ , which is a preliminary mean DOT over the ocean segment.) Sea surface height uncertainty,  $h\_uncrtn$ , as well as the photon rate ( $photon\_rate$ ) and the photon noise rate ( $photon\_noise\_rate$ ) are also gridded. See Table 3 for complete list of ATL19 variables.

<sup>\*</sup>Reminder: In ATL12 processing to reduce variability due to the considerable non-oceanographic variation in the geoid, we work with DOT, the anomaly of photon heights about the geoid. ATL12 outputs sea surface height,  $h$ , relative to the WGS84 ellipsoid to be consistent with other ICESat output. For ATL12 output, ocean segment DOT is converted to mean sea surface height,  $h$ , by adding ocean segment mean geoid height,  $geoid\_seg$ , which is also output by ATL12.

For gridding purposes, ATL12 provides the number of photon heights,  $n\_photons$ , in each ocean segment used to determine the DOT moments. It also provides the effective degrees-of-freedom,  $np\_effect$ , which are based on the correlation length scale of surface heights and allow computing grid averages weighted by degrees of freedom. See Table 3 for complete list of ATL19 variables.

#### **3.2.3.1 Pre-grid Filtering – Along-Track**

We find that for reasons that we are investigating, ATL12 produces some ocean segment heights that are unrealistic compared to the geoid. In the first release of ATL19, heights,  $h$ , that do not survive a 2-pass 3-sigma filter on dynamic ocean topography (DOT equal to  $h-geoid\_seg$ ) are edited out from being used in ATL19 computations. This results in rejection of some good data, particularly in the Southern Ocean where the mean DOT is low. In the future, for each 4-orbit ATL12 file, data from all six beams are concatenated. Means of dynamic ocean topography (DOT equal to  $h-geoid\_seg$ ) are computed for each of the 18 ten-degree latitude bands for an ATL12 file. The latitude bands are centered on the 5° marks and do not overlap, i.e. {90°S ≤ ATL12 latitudes < 85°S}, {85°S ≤ ATL12 latitudes < 80°S}, ... {80°N ≤ ATL12 latitudes < 75°N}. The standard

deviation,  $\sigma$ , of the DOT from the entire ATL12 file is also computed, and DOTs that are outside of  $\pm 3\sigma$  from the associated latitude-band mean, are removed.

**Table 1 Inputs to ATL19 from ATL12**  
**(See Table 6 in ATL12 ATBD for all ATL12 Outputs)**

<b>Product Label</b>	<b>Units</b>	<b>Description</b>	<b>Symbol</b>
<b>gtx/ssh_segments /</b>			
<i>latitude</i>	degrees	Mean latitude of surface photons in segment	<b><i>lat_seg</i></b>
<i>longitude</i>	degrees	Mean longitude of surface photons in segment	<b><i>lon_seg</i></b>
<b>gtx/ssh_segments /heights</b>			
<i>h</i>	meters	Mean sea surface height relative to the WGS84 ellipsoid	<b><i>SSH</i></b>
<i>h_var</i>	meters <sup>2</sup>	Variance of best fit probability density function (meters <sup>2</sup> )	<b><i>SSHvar</i></b>
<i>h_skewness</i>		Skewness of photon sea surface height histogram	<b><i>SSHskew</i></b>
<i>h_kurtosis</i>		<i>Excess kurtosis of sea surface height histogram</i>	<b><i>SSHkurt</i></b>
<i>meanoffit2</i>	meters	Mean of linear fit removed from surface photon height expressed as DOT during surface finding	<b><i>meanoffit2</i></b>
<i>y</i>	m <sup>-1</sup>	Probability density function of photon surface height	<b><i>Y</i></b>
<i>length_seg</i>	meters	Length of segment (m)	<b><i>length_seg</i></b>
<i>binsize</i>	meters	Bin size for Y and sshx	<b><i>binsize</i></b>
<i>bin_ssbias</i>	meters	Sea state bias estimated from the correlation of photon return rate with along track 10-m bin averaged surface height.	<b><i>binSSBias</i></b>
<i>swh</i>	meters	Significant wave height estimated as 4 times the standard deviation of along track 10-m bin averaged surface height	<b><i>SWH</i></b>
<i>xbin</i>	meters	Center of 1 x 710 element array of 10-m bins. Note this may be included as a	<b><i>xbin</i></b>

		data description or other static array equal to [5, 15, 25, 35 ..... 7095 m]	
<i>xbind</i>	meters	1 x 710 element array of potential 10-m bin averages of along-track distance	<b><i>xbind</i></b>
<i>h_uncrtn</i>	meters	Uncertainty in the mean sea surface height over an ocean segment	<b><i>h_uncrtn</i></b>
<i>np_effect</i>		Effective degrees of freedom of the average sea surface height for the ocean segment	<b><i>NP_effect</i></b>
<i>l_scale</i>		Correlation length scale expressed as a number of 10-m bins	<b><i>Lscale</i></b>
<i>nbin10</i>		Number of 10-m bins in an ocean segment	<b><i>Nbin10</i></b>
<b>gtx/ssh_segments/stats</b>			
<i>n_photons</i>		Number of surface photons found for the segment	<b><i>n_photon</i></b>
<i>n_ttl_photon</i>		Total number of photons in the downlink band for the segment	<b><i>n_ttl_photon</i></b>
<i>depth_ocn_seg</i>	meters	The average of depth ocean of geo-segments used in the ocean segment.	<b><i>depth_ocn_seg</i></b>
<i>geoid_seg</i>	meters	Ocean segment average of geoid height above the WGS - 84 reference ellipsoid (range -107 to 86 m)	<b><i>geoid_seg</i></b>
<i>surf_type_prcnt</i>		The percentages of each <i>surf_type</i> of the photons in the ocean segment as a 5-element variable with each element corresponding to the percentage of photons from each of the 5 surface types	<b><i>surf_type_prcnt</i></b>
<b>ancillary_data/</b>			
<i>ds_y_bincenters</i>	meters	Bin centers for <i>y</i> probability density function -15 to +15, by 1cm bins	

### 3.2.4 Gridding

The ATL19 gridding process involves three general steps: binning, averaging, and interpolation to grid cell center. There are two averaging methods; simple averaging, and

averaging weighted by the number of degrees of freedom of the ocean segment data. Data interpolated to grid cell center are also included in the ATL19 data product.

### **3.2.4.1 Binning**

Consider one month of ATL12 concatenated data for each beam. Using the latitude and longitude from ATL12, *lat\_seg*, and *lon\_seg*, find the data that fall within a grid cell. For the polar grids, first convert the latitude and longitude to the appropriate polar stereographic coordinates *x\_seg* and *y\_seg* using libraries located at: [https://nsidc.org/data/polar-stereo/tools\\_geo\\_pixel.html](https://nsidc.org/data/polar-stereo/tools_geo_pixel.html) with coordinate transforms for lat, lon to x, y and x, y to lat, lon also given in Appendix D. The appropriate grid bin containing each ocean segment can then be identified based on *x\_seg* and *y\_seg* and the x and y boundaries of the grid cells. Once the correct bin is identified, the data corresponding to Table 1 for that ocean segment is accumulated. This will result in each grid cell having a collection of the data from all *n\_segs* ocean segments contained in the grid cell for each beam (*beam\_1*, *beam\_2*, etc).

Once the ocean segments appropriate to each bin are identified, compute *n\_ph\_srfc*, the sum of the number of surface reflected photons, *n\_photons*, for all ocean segments in the grid cell. Also compute *n\_phs\_ttl* as the grid cell-total of all photons in the downlink bands, *n\_ttl\_photon*. Compute *dof* equal to the sum of all the *NP\_effect* in the bin. Compute the total length of all ocean segments in the bin, *length\_sum*, as the sum of *length\_seg*. Also output the number of segments in the bin, *n\_segs*. Additionally, compute the grid cell-aggregate photon rate, *r\_srfc*, equal to *n\_ph\_srfc* divided by the total length of segments in the bin, *length\_sum*. Finally, compute the grid cell noise rate, *r\_noise*, equal to (*n\_phs\_ttl* minus *n\_ph\_srfc*) divided by *length\_sum*.

### **3.2.4.2 Individual Beam Averaging**

#### **3.2.4.2.1 Averaging over *n\_segs* Segments**

For each grid cell and each beam with the accumulated data of *n\_segs* ocean segments compute outputs:

*dot\_avg*, *lat\_avg*, *lon\_avg*, *ssb\_avg*, *geoid\_avg*, *depth\_avg*, and *surf\_type\_prcnt*

as simple averages of:

*SSH-geoid\_seg*, *lat\_seg*, *lon\_seg*, *bin\_ssbias*, *geoid\_seg*, *depth\_ocn\_seg*, and *surf\_prcnt\_avg*.

Simple average is defined by the sum of the *n\_segs* ocean segment values of these variables divided by *n\_segs*. See Figure 5 for the August 2020 strong Beam-1 (Fig. 5 left) and strong Beam-3 (Fig. 5 right) “*n-segs*” averages, from our Matlab developmental code.

To compute the bin average standard deviation, *dot\_sigma\_avg*, of DOT variability over ocean segments, sum *SSHvar*, divide by *n\_segs*, and take the square root to establish the average standard deviation. Note that this and the other average moments do not

include the ocean-segment-to-ocean-segment variability within the cell. This is likely much smaller than the variability due to sea state, but in future releases we plan to distinguish the ocean-segment-to-ocean-segment variability where adequate ocean segments are included by a TBD method.

Similarly, to compute the bin average significant wave height, *SWH\_avg*, sum  $(SWH)^2$ , divide by *n\_segs*, and take the square root to establish the average significant wave height.

To compute the bin average skewness, *dot\_skew\_avg*, of DOT, sum  $SSHskew \times (SSHvar)^{3/2}$ , divide by *n\_segs*, and divide by  $dot\_sigma\_avg^3$  to establish the average skewness.

To compute the bin average excess kurtosis, *dot\_kurt\_avg*, of DOT, sum  $(SSHkurt+3) \times (SSHvar)^2$ , divide by *n\_segs*, and divide by  $dot\_sigma\_avg^4$ . Subtract 3 to establish the average excess kurtosis.

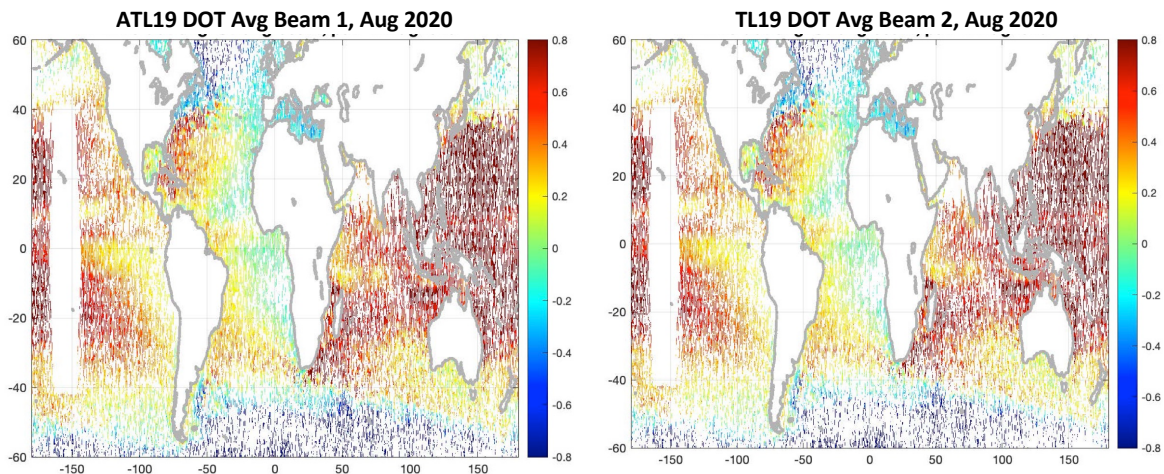


Figure 5. Mid-latitude grid averages of DOT strong beams, Beam 1 (left) and Beam 2 (right), August 2020. Average DOT differences: beam2 – beam1 = 0.61 cm, beam3 – beam1 = 0.55 cm, beam2 – beam3 = -0.08 cm. The blank rectangle in the Central Pacific is the region of ocean-scans not gridded according to the pointing and orbit determination flag.

To compute the uncertainty, *dot\_avg\_uncrtn*, in gridded DOT, *dot\_avg*, divide  $dot\_sigma\_avg$  by the square root of *dof* to establish the uncertainty in the degree-of-freedom weighted DOT. As with the higher moments, this is the uncertainty due to sea state and does not include the ocean-segment-to-ocean-segment variability within the cell. In future releases we plan to estimate the ocean-segment-to-ocean-segment uncertainty where adequate ocean segments are included by a TBD method.

To compute the bin aggregate probability density function (PDF), *dot\_hist*, of DOT, we first must convert each *Y* PDF from ATL12 to a PDF of DOT by adding *meanoffit2* to the x-axis of *Y*, *ds\_y\_bincenters* and then interpolating the result to an intermediate PDF,

*Yintermediate*, evaluated at the original *ds\_y\_bincnters*. (Note: In ATL19 Release 1, *meanoffit2* was inadvertently not added so the aggregate histograms only reflect the aggregate wave environment with mean near zero.) The aggregate probability PDF, *dot\_hist*, of DOT will equal the sum *Yintermediate x n\_photons* in each histogram bin of all *Yintermediate* divided by the total, *n\_photons\_gridttl*, of all *n\_photons*.

**Table 2: Mid-Latitude Inter-Beam Biases, Oct. & Nov. 2020**

No Ocean Scans	Beam 1	Beam 2	Beam 3	Beam 4	Beam 5	Beam 6
Beam 1		0.0066	0.0066	0.0021	0.0066	-0.0089
Beam 2	-0.0066		-0.0024	-0.0017	0.0024	-0.0107
Beam 3	-0.0066	0.0024		-0.0001	-0.0001	-0.0116
Beam 4	-0.0021	0.0017	0.0001		0.0041	-0.0096
Beam 5	-0.0066	-0.0024	0.0001	-0.0041		-0.0152
Beam 6	0.0089	0.0107	0.0116	0.0096	0.0152	

**3.2.4.2.2 Averaging Weighted by Degrees-of-Freedom**

To account for the different uncertainties in linear variables (e.g., DOT) the averaging is as in 5.6.4.2 except the variables are weighted by the effective degrees of freedom, *NP\_effect*, of each ocean segment DOT. These degree-of-freedom weighted averages may be different from simple averages in important ways for cases where different beams in a cell measure over different sea states and have different sea state induced DOT uncertainty. DOT measured under calm conditions will be more certain than DOT measured over a rough sea surface.

For each grid cell and each beam with the accumulated data of *n\_segs* ocean segments compute outputs

*dot\_dfw, lat\_dfw, lon\_dfw, ssb\_dfw, geoid\_dfw, and depth\_dfw*

as degree-of-freedom weighted averages of :

*SSH- geoid\_seg, lat\_seg, lon\_seg, bin\_ssbias, geoid\_seg, depth\_ocn\_seg, length\_seg, and surf\_type\_prcnt.*



Degree-of-freedom averages are found by first taking the sum of the *n\_segs* ocean segment values multiplied by their respective ocean segment *NP\_effect* and then dividing by *dof*, which is equal to the sum of all the *NP\_effect* in the bin to establish the degree-of-freedom weighted averages.

To compute the bin degree-of-freedom weighted average standard deviation of DOT, *dot\_sigma\_dfw*, of DOT, sum *SSHvar* multiplied by *NP\_effect*. Then divide by *dof* and take the square root to establish the degree-of-freedom weighted standard deviation of DOT. Note that this and the other average moments do not include the ocean-segment-to-ocean-segment variability within the cell. This is likely much smaller than the variability due to sea state, but in future releases we plan to distinguish the ocean-segment-to-ocean-segment variability where adequate ocean segments are included by a TBD method.

Similarly, to compute the bin degree-of-freedom weighted average significant wave height, *SWH\_dfw*, sum  $(SWH)^2$  multiplied by *NP\_effect*. Then divide by *dof* and take the square root to establish the degree-of-freedom weighted average significant wave height.

To compute the bin degree-of-freedom weighted average skewness, *dot\_skew\_dfw*, of DOT, sum *SSHskew* x  $(SSHvar)^{3/2}$ , multiplied by *NP\_effect*. Then divide by *dof* and divide again by *dot\_sigma\_dfw*<sup>3</sup> to establish the degree-of-freedom weighted skewness.

To compute the bin degree-of-freedom weighted average excess kurtosis, *dot\_kurt\_dfw*, of DOT, sum  $(SSHkurt+3)$  x  $(SSHvar)^2$  multiplied by *NP\_effect*. Then divide by *dof* and divide again by *dot\_sigma\_dfw*<sup>4</sup>. Subtract 3 to establish the degree-of-freedom weighted excess kurtosis.

To compute the uncertainty, *dot\_dfw\_uncrtn*, in gridded DOT, *dot\_dfw*, divide *dot\_sigma\_dfw* by the square root of *dof* to establish the uncertainty in the degree-of-freedom weighted DOT. As with the higher moments, this is the uncertainty due to sea state and does not include the ocean-segment-to-ocean-segment variability within the cell. In future releases we plan to estimate the ocean-segment-to-ocean-segment uncertainty where adequate ocean segments are included by a TBD method.

### **3.2.4.2.3 Inter-Beam Biases**

The procedures of section 3.2.4.2 will be performed independently for each beam, if for no other reason than a particular satellite pass may have ground tracks in adjacent pairs of cells. Furthermore, comparing the gridded product for the individual beams will disclose instrumental biases. For example, for August 2020, biases between the strong beams were significantly less than a centimeter (Figure 5), and Table 2 shows that the mid-latitude grid average inter-beam biases for October-November 2020 were mostly less than a centimeter. In the future inter-beam biases can be monitored with gridded single-beam averages and accounted for by a TBD method in a gridded product that combines all the beams.

### 3.2.4.3 All-beam Averages

We want all-beam quantities for each grid cell to achieve grid cell averages with maximum degrees of freedom and minimum uncertainty. Figure 6 shows DOT gridded by our developmental code in the mid-latitude grid by simple averaging (left) and degree-of-freedom weighted averaging (right).

All-beam quantities will mirror the single beam totals and averages of section 3.2.4.2 and use the same names with the suffix “*\_albm*” appended (See Table 3). The all-beam variables are computed in the same way the single beam variables are computed except all the ocean segments from all beams in a grid cell are used in the computation. These values should be the same as appropriately weighted averages of grid cell single beam averages (See Appendix D).

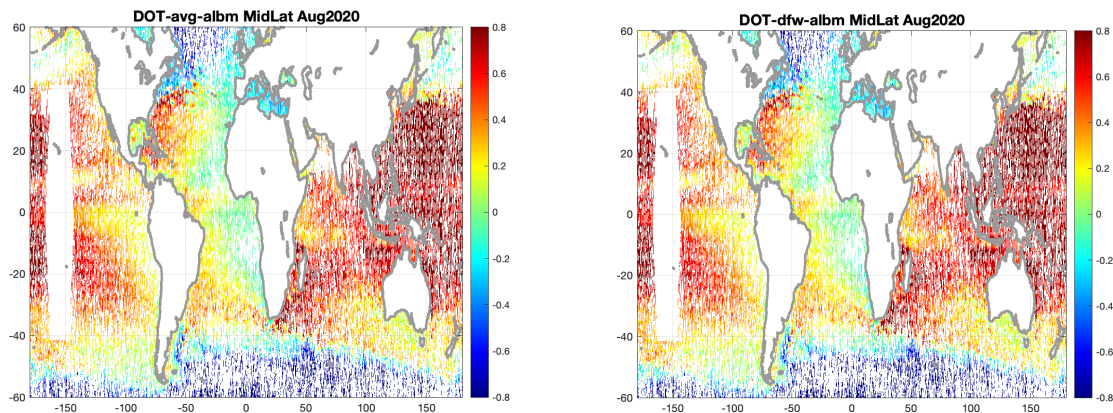


Figure 6. Mid-latitude DOT gridded by simple “n-segment” all-beam averages (left) and degree-of-freedom weighted (dfw) all-beam averages (right) for August 2020. The ocean scan region in the Central Pacific is not gridded.

### 3.2.4.4 Interpolation of DOT to Bin Centers

To compute the average DOT at the center of each grid cell, we perform a least squares fit of a plane of the form  $dot = a * x + b * y + c$  to the ocean segment DOT in each cell and evaluate the fitted plane at the center of the cell. For a sensible solution we require data from at least two ICESat-2 orbits. Due to the spacing of the orbits we look for data in nine cells; the center cell where we will compute the center-interpolated value and the eight cells surrounding that center cell. There must also be a minimum of three ocean segments in the cell to compute a center-interpolated DOT value.

#### 3.2.4.4.1 Average DOT at Bin Centers

Computing averages interpolated to grid cell centers requires data from at least two orbits to get the required horizontal distribution of data to make a meaningful least squares fit in

space. The ICESat-2 orbital characteristics require that for a 1-month average at a grid cell center we must consider data in the surrounding 8 cells for a 9-cell fit.

For **n\_segs** greater than or equal to 3 from at least two orbits, assemble 1 by **n\_segs** vectors of the deviation of the DOT values from their average values, **dot\_avg9**, **lon\_avg9**, and **lat\_avg9**, where we are including the data from all nine cells for those averages.

$$h_i' = (\text{SSH-geoid\_seg}) - \text{dot\_avg9} \quad i = 1 \text{ to } n\_segs \quad (45)$$

$$x_i' = \text{lon\_seg} - \text{lon\_avg9} \quad i = 1 \text{ to } n\_segs \quad (46)$$

$$y_i' = \text{lat\_seg} - \text{lat\_avg9} \quad i = 1 \text{ to } n\_segs \quad (47)$$

Referring to Appendix B, compute the cross product expected values  $L_{xx}$ ,  $L_{yy}$ ,  $L_{xy}$ ,  $R_{xh}$ , and  $R_{yh}$ :

$$\begin{aligned} L_{xx} &= \sum_{i=1}^N x_i' x_i' \\ L_{yy} &= \sum_{i=1}^N y_i' y_i' \\ L_{xy} &= \sum_{i=1}^N y_i' x_i' \end{aligned} \quad \text{and} \quad \begin{aligned} R_{xh} &= \sum_{i=1}^N x_i' h_i' \\ R_{yh} &= \sum_{i=1}^N y_i' h_i' \end{aligned} \quad (48)$$

for  $N$  equal to **n\_segs**.

The coefficients defining the least-squares planar fit  $a$ ,  $b$ , and  $c$  are given by

$$\begin{aligned} a &= \frac{R_{xh} L_{yy} - R_{yh} L_{xy}}{L_{xx} L_{yy} - L_{xy}^2} \\ b &= \frac{R_{yh} L_{xx} - R_{xh} L_{xy}}{L_{xx} L_{yy} - L_{xy}^2} \\ c &= \text{dot\_avg9} - (a * \text{lon\_avg9} + b * \text{lat\_avg9}) \end{aligned} \quad (49)$$

The value of **dot\_avg** interpolated to the center of the grid cell, **dot\_avgcntr** is then given by:

$$\text{dot\_avgcntr} = a * \text{gridcntr\_lon} + b * \text{gridcntr\_lat} + c \quad (50)$$

Center values are also calculated for depth, geoid, sea state bias and significant wave height as well as DOT, all variable names ending in **\_avgcntr**.

#### 3.2.4.4.2 Degree-of-Freedom Averaged DOT at Bin Centers

Similarly, to compute the average of degree-of-freedom weighted DOT at the center of each grid cell, assemble 1 by **n\_segs** vectors of the deviation of the DOT values from their

degree-of-freedom weighted average values,  $dot\_dfw9$ ,  $lon\_dfw9$ , and  $lat\_dfw9$ , again using data from 9 (3x3) cells.

$$h_i' = (NP\_effect)^{1/2} * (SSH - geoid\_seg - dot\_dfw9) \quad i= 1 \text{ to } n\_segs \quad (51)$$

$$x_i' = (NP\_effect)^{1/2} * (lon\_seg - grid\_lon\_dfw9) \quad i= 1 \text{ to } n\_segs \quad (52)$$

$$y_i' = (NP\_effect)^{1/2} * (lat\_seg - grid\_lat\_dfw9) \quad i= 1 \text{ to } n\_segs \quad (53)$$

$(NP\_effect)^{1/2}$  instead of  $NP\_effect$  above because in the next cross product calculation the multiplication is to amplify the sums by factors of  $NP\_effect$  as if the number of DOT values and their locations were expanded to number  $NP\_effect$ . Referring to Appendix D, compute

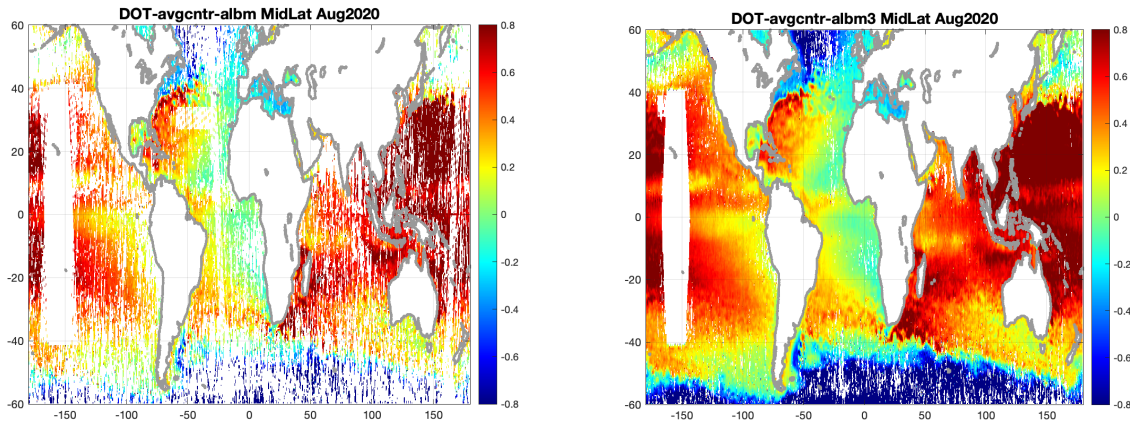


Figure 7. Centered grid averages using 9-cells (3x3) to fit to the center of a center cell for 1-month, August 2020, (left) and 3-months, Jul-Aug-Sept. 2020, (right).

the cross product expected values  $L_{xx}$ ,  $L_{yy}$ ,  $L_{xy}$ ,  $R_{xh}$ , and  $R_{yh}$  using equations (48) for  $N$  equal to  $do_f$  equal to the sum of all the  $NP\_effect$  in the 9 bins.

The coefficients defining the least-squares planar fit ( $a$ ,  $b$ , and  $c$ ) are given by (49) with the exception that  $c = dot\_dfw9 - (a * lon\_dfw9 + b * lat\_dfw9)$ . The degree-of-freedom weighted value of  $dot\_dfw$  interpolated to the center of the grid cell,  $dot\_dfwcntr$  is then given by:

$$dot\_dfwcntr = a * gridcntr\_lon + b * gridcntr\_lat + c \quad (54)$$

Center values will also be calculated for depth, geoid, sea state bias and significant wave height as well as DOT, all variable names ending in  $_dfwcntr$ .

### 3.2.4.4.3 One-month and Three-month Centered Averages

Figure 6 shows DOT grid averages interpolated to cell centers using Equations (45)-(50) for 1-month, August 2020, (Figure 7, left) and 3-months, Jul.-Aug.-Sept. 2020, (Figure 7, right). The results are similar for degree-of-freedom averaging Section 3.2.4.4.2, Equations

(51)-(54). Even at 1-month, the spatial averaging of the 9-cell fit results in significantly fewer empty cells than the simple averages (Figure 6, left). Furthermore, the 91-day repeat of ICESat-2 including 1397 orbits, with two equator crossings per orbit each, results in an equator crossing every 0.13 degrees of longitude, so that every  $\frac{1}{4}^\circ$  grid cell has the potential, barring clouds, to see at least one satellite pass in 3 months. Consequently, almost every grid cell is filled in the 3-month centered average for July-Sept. 2020 (Figure 7, right). The 3-month centered average (Fig. 7, right) and degree-of-freedom weighted average will be good candidate background fields for optimal interpolation to finer spatial and temporal scales (Appendix E).

### 3.2.5 Gridding Output

Output of the ATL19 gridding process will come in three latitude groups: mid-latitude, north-polar, and south-polar for the three grid systems (Section 3.2.1). A hierarchy of the ATL12 and ATL19 variables is given in Appendix D. The generic list of output variables applicable to each latitude group is given in Table 3. The grid sizes vary with region: mid-latitude [480 x 1440] (y-index, x-index), north-polar [448 x 304] and south-polar [332 x 316].

**Table 3: ATL19 Outputs per Latitude Group**

As indicated by “\_”\_ *albm*, *albm* versions of the variables are also included

\* Indicates in single beam groups only

ATL19 Variable Name	Dimensions mid-lat, north-polar, south-polar	Units	Description	Input ATL12 Variable Name
<i>delta_time_beg</i>	1	seconds	Earliest time in grid	<i>delta_time</i>
<i>delta_time_end</i>	1	seconds	Latest time in grid	<i>delta_time</i>
<i>depth_avg</i> “_”_ <i>albm</i>	480 x 1440 448 x 304 332 x 316 INVALID_R8B	meters	Simple average of ocean depth	<i>depth_ocn_seg</i>
<i>depth_avgcntr</i> “_”_ <i>albm</i>	480 x 1440 448 x 304 332 x 316 INVALID_R8B	meters	Simple average of ocean depth at center of grid cell	<i>depth_ocn_seg</i>
<i>depth_dfw</i> “_”_ <i>albm</i>	480 x 1440 448 x 304 332 x 316 INVALID_R8B	meters	Degree of freedom weighted average of ocean depth	<i>depth_ocn_seg</i>
<i>depth_dfwcntr</i>	480 x 1440	meters	Degree of freedom weighted	<i>depth_ocn_seg</i>

*ICESat-2 Algorithm Theoretical Basis Document for Gridded Dynamic Ocean Topography*

**Release 001**

<i>“_”_albm</i>	448 x 304 332 x 316 INVALID_R8B		average of ocean depth at center of grid cell	
<i>dof</i> <i>dof_albm</i>	480 x 1440 448 x 304 332 x 316	counts	Sum of degrees of freedom	<i>np_effect</i>
<i>dot_avg</i> <i>“_”_albm</i>	480 x 1440 448 x 304 332 x 316 INVALID_R8B	meters	Simple average of dynamic ocean topography	<i>h-geoid_seg</i>
<i>dot_avg_uncrtn</i> <i>“_”_albm</i>	480 x 1440 448 x 304 332 x 316 INVALID_R8B	meters	Uncertainty average of dynamic ocean topography	<i>np_effect</i> <i>h_var</i>
<i>dot_avgcntr</i> <i>“_”_albm</i>	480 x 1440 448 x 304 332 x 316 INVALID_R8B	meters	Simple average of dynamic ocean topography interpolated to center of grid cell	<i>h-geoid_seg</i>
<i>dot_dfw</i> <i>“_”_albm</i>	480 x 1440 448 x 304 332 x 316 INVALID_R8B	meters	Degree of freedom weighted average of the dynamic ocean topography	<i>h-geoid_seg</i>
<i>dot_dfw_uncrtn</i>	480 x 1440 448 x 304 332 x 316 INVALID_R8B	meters	Degree of freedom weighted average of dynamic ocean topography uncertainty	<i>h_uncrtn</i>
<i>dot_dfwcntr</i> <i>“_”_albm</i>	480 x 1440 448 x 304 332 x 316 INVALID_R8B	meters	Degree of freedom weighted average dynamic ocean topography interpolated to center of grid cell	<i>h-geoid_seg</i>
<i>dot_hist</i>	480 x 1440 448 x 304 332 x 316 INVALID_R4B	counts	Single beam aggregate probability density function of DOT from photon heights histograms	<i>y</i>
<i>dot_hist_albm</i>	480 x 1440 448 x 304 332 x 316 INVALID_R4B	counts	All beam aggregate probability density function of DOT from photon heights histograms	<i>y</i>
<i>dot_kurt_avg*</i>	480 x 1440	none	Simple average of excess	<i>h_kurtosis</i>

	448 x 304 332 x 316 INVALID_R8B		kurtosis of the dynamic ocean topography	
<i>dot_kurt_dfw*</i>	480 x 1440 448 x 304 332 x 316 INVALID_R8B	none	Degree of freedom weighted average of excess kurtosis of the dynamic ocean topography	<i>h_kurtosis</i>
<i>dot_sigma_avg</i> “_”_albm	480 x 1440 448 x 304 332 x 316 INVALID_R8B	meters	Simple average of the standard deviation of dynamic ocean topography	<i>h_var</i>
<i>dot_sigma_dfw</i> “_”_albm	480 x 1440 448 x 304 332 x 316 INVALID_R8B	meters	Degree of freedom weighted average of the standard deviation of the dynamic ocean topography	<i>h_var</i>
<i>dot_skew_avg*</i>	480 x 1440 448 x 304 332 x 316 INVALID_R8B	none	Simple average of the skewness of dynamic ocean topography	<i>h_skewness</i>
<i>dot_skew_dfw*</i>	480 x 1440 448 x 304 332 x 316 INVALID_R8B	none	Degree of freedom weighted average of the skewness of dynamic ocean topography	<i>h_skewness</i>
<i>ds_grid_x</i>	304 (N) 316 (S)	meters	Center x value of polar grid cell	defined
<i>ds_grid_y</i>	448 (N) 332 (S)	meters	Center y value of polar grid cell	defined
<i>geoid_avg</i> “_”_albm	480 x 1440 448 x 304 332 x 316 INVALID_R8B	meters	Simple average of geoid height	<i>geoid_seg</i>
<i>geoid_avgcntr</i> “_”_albm	480 x 1440 448 x 304 332 x 316 INVALID_R8B	meters	Simple average of geoid height interpolated to center of grid cell	<i>geoid_seg</i>
<i>geoid_dfw</i> “_”_albm	480 x 1440 448 x 304 332 x 316 INVALID_R8B	meters	Degree of freedom weighted average of geoid height	<i>geoid_seg</i>
<i>geoid_dfwcntr</i> “_”_albm	480 x 1440 448 x 304 332 x 316 INVALID_R8B	meters	Degree of freedom weighted average of geoid height interpolated to center of grid	<i>geoid_seg</i>

*ICESat-2 Algorithm Theoretical Basis Document for Gridded Dynamic Ocean Topography*

**Release 001**

			cell	
<i>gridcntr_lat</i>	480 x 1440 448 x 304 332 x 316	°N	Latitude of grid cell center	defined
<i>gridcntr_lon</i>	480 x 1440 448 x 304 332 x 316	°E	Longitude of grid cell center	defined
<i>latitude</i>	480	°N	Vector of grid center latitude common values for all mid- latitude grid cells	defined
<i>lat_avg</i> “_”_albm	480 x 1440 448 x 304 332 x 316 INVALID_R8B	°N	Simple average of latitude	<i>latitude</i>
<i>lat_dfw</i> “_”_albm	480 x 1440 448 x 304 332 x 316 INVALID_R8B	°N	Degree of freedom weighted average of latitude	<i>latitude</i>
<i>length_sum</i> “_”_albm	480 x 1440 448 x 304 332 x 316 INVALID_R8B	meters	Sum of ocean segment lengths	<i>length_seg</i>
<i>longitude</i>	1440	°E	Vector of all center longitude common values for all mid- latitude grid cell	defined
<i>lon_avg</i> “_”_albm	480 x 1440 448 x 304 332 x 316 INVALID_R8B	°E	Simple average of longitude	<i>longitude</i>
<i>lon_dfw</i> “_”_albm	480 x 1440 448 x 304 332 x 316 INVALID_R8B	°E	Degree of freedom weighted average of longitude	<i>longitude</i>
<i>n_ph_srfc</i> “_”_albm	480 x 1440 448 x 304 332 x 316 INVALID_I8B	counts	Sum of surface reflected photons	<i>n_photons</i>
<i>n_phs_ttl</i> “_”_albm	480 x 1440 448 x 304 332 x 316 INVALID_I8B	counts	Sum of surface reflected photons plus rejected photons	<i>n_ttl_photon</i>
<i>n_segs</i>	480 x 1440	counts	Number of ocean segments	



<i>“_”_albm</i>	448 x 304 332 x 316 INVALID_I4B		in grid cell	
<i>r_noise</i> <i>“_”_albm</i>	480 x 1440 448 x 304 332 x 316 INVALID_R8B	count/ meter	Simple average of photon noise rate	<i>photon_noise_rate</i>
<i>r_srfc</i> <i>“_”_albm</i>	480 x 1440 448 x 304 332 x 316 INVALID_R8B	count/ meter	Simple average of surface reflected photon rate	<i>photon_rate</i>
<i>sea ice flag</i> (tbd )	480 x 1440 448 x 304 332 x 316		Indication of the fraction of ocean segments that fall under the passive microwave derived sea ice mask of ATL20	TBD
<i>surf_prcnt_avg</i> <i>“_”_albm</i>	5x[ 480 x 1440 448 x 304 332 x 316]	percent	The averages of the percentages of each <b>surface</b> type in the grid cell ocean segment as a 5-element variable with each element corresponding to the percentage of each of the 5 surface types.	<i>surf_type_prcnt</i>
<i>ssb_avg</i> <i>“_”_albm</i>	480 x 1440 448 x 304 332 x 316 INVALID_R8B	meters	Simple average of sea state bias	<i>bin_ssbias</i>
<i>ssb_avgcntr</i> <i>“_”_albm</i>	480 x 1440 448 x 304 332 x 316 INVALID_R8B	meters	Simple average of sea state bias interpolated to center of grid cell	<i>bin_ssbias</i>
<i>ssb_dfw</i> <i>“_”_albm</i>	480 x 1440 448 x 304 332 x 316 INVALID_R8B	meters	Degree-of-freedom weighted average of sea state bias	<i>bin_ssbias</i>
<i>ssb_dfwcntr</i> <i>“_”_albm</i>	480 x 1440 448 x 304 332 x 316 INVALID_R8B	meters	Degree-of-freedom weighted average of sea state bias interpolated to center of grid cell	<i>bin_ssbias</i>
<i>swh_avg</i>	480 x 1440	meters	Simple average of the	<i>swh</i>

"_ "_albm	448 x 304 332 x 316 INVALID_R8B		significant wave height	
swh_avgcnt "_"_albm r	480 x 1440 448 x 304 332 x 316 INVALID_R8B	meters	Simple average of the significant wave height interpolated to center of grid cell	swh
swh_dfw "_"_albm	480 x 1440 448 x 304 332 x 316 INVALID_R8B	meters	Degree of freedom weighted average of the significant wave height	swh
swh_dfwcntr "_"_albm	480 x 1440 448 x 304 332 x 316 INVALID_R8B	meters	Degree of freedom weighted average of the significant wave height interpolated to center of grid cell	swh
<b>ancillary_data/</b>				
ds_y_bincenters	1x3001	meters	Bin centers for y probability density function -15 to +15, by 1cm bins	

**References**

Morison, J. H., D. Hancock, S. Dickinson, J. Robbins, L. Roberts, R. Kwok, S. Palm, B. Smith, M. Jasinski, and I.-S. Team. (2019), ATLAS/ICESat-2 L3A Ocean Surface Height, Version 2Rep., NASA National Snow and Ice Data Center Distributed Active Archive Center, Boulder, Colorado USA..

Neumann, T. A., A. Brenner, D. Hancock, J. Robbins, J. Saba, K. Harbeck, A. Gibbons, J. Lee, S. B. Luthcke, T. Rebold, et al. (2021a). ATLAS/ICESat-2 L2A Global Geolocated Photon Data, Version 4. [Indicate subset used]. Boulder, Colorado USA. NASA National Snow and Ice Data Center Distributed Active Archive Center. doi: <https://doi.org/10.5067/ATLAS/ATL03.004>.

Luthcke, and T. Rebold (2021b), ICESat-2 Algorithm Theoretical Basis Document (ATBD) for Global Geolocated Photons ATL03, [https://nsidc.org/sites/nsidc.org/files/technical-references/ICESat2 ATL03 ATBD r004.pdf](https://nsidc.org/sites/nsidc.org/files/technical-references/ICESat2_ATL03_ATBD_r004.pdf)

## **ACRONYMS**

ASAS	ATLAS Science Algorithm Software
ATLAS	ATLAS Advance Topographic Laser Altimeter System
GSFC	Goddard Space Flight Center
ICESat-2 MIS	ICESat-2 Management Information System
IIP	Instrument Impulse Response
MIZ	Marginal Ice Zone
PSO	Project Science Office
PSO	ICESat-2 Project Support Office
SDMS	Scheduling and Data Management System
SIPS	Science Investigator-led Processing System
TEP	Transmit Echo Pulse

## **GLOSSARY**

**APPENDIX A: ICESat-2 Data Products**

ICESat-2 Data Products

<b>File ID/Level</b>	<b>Product Name</b>	<b>Concept</b>	<b>Short Description</b>	<b>Frequency</b>
00/0	Telemetry Data	Full rate Along-track with channel info	Raw ATLAS telemetry in Packets with any duplicates removed	Files for each APID for some defined time period
01/1A	Reformatted Telemetry	Full rate Along-track with channel info	Parsed, partially reformatted, time ordered telemetry. Proposed storage format is NCSA HDF5.	Uniform time TBD minutes (1 minute?)
02/1B	Science Unit Converted Telemetry	Full rate Along-track with channel info	Science unit converted time ordered telemetry. Reference Range/Heights determined by ATBD Algorithm using Predict Orbit and s/c pointing. All photon events per channel per pulse. Includes Atmosphere raw profiles.	Uniform time TBD minutes (1 minute?)
03/2A	Global Geolocated Photon Data	Full rate Along-track with channel info	Reference Range/Heights determined by ATBD Algorithm using POD and PPD. All photon events per pulse per beam. Includes POD and PPD vectors. Classification of each photon by several ATBD Algorithms.	Uniform time TBD minutes (1 minute?)
04/2A	Calibrated Backscatter Profiles	3 profiles at 25 Hz rate (based on 400 pulse mean)	Along-track backscatter data at full instrument resolution. The product will include full 532 nm (14 to -1.0 km) calibrated attenuated backscatter profiles at 25 times per second for vertical bins of approximately 30 meters. Also included will be calibration coefficient values for the polar region.	Per orbit
05/2B	Photon Height Histograms	Fixed distances Along-track for each beam	Histograms by prime Classification by several ATBD Algorithms. By beam	Uniform time TBD minutes (30 minutes?)
06/L3	Antarctica Ice Sheet Height / Greenland Ice Sheet Height	Heights calculated with the ice sheet algorithm, as adapted for a dH/dt calculation	Surface heights for each beam, along and across-track slopes calculated for beam pairs. All parameters are calculated for the same along-track increments for each beam and repeat.	There will be TBD files for each ice sheet per orbit

**ICESat-2 Algorithm Theoretical Basis Document for Gridded Dynamic Ocean Topography**

**Release 001**

<b>File ID/Level</b>	<b>Product Name</b>	<b>Concept</b>	<b>Short Description</b>	<b>Frequency</b>
07/ L3	Arctic Sea Ice Height/ Antarctic Sea Ice Height	Along-track heights for each beam ~50-100m (uniform sampling); separate Arctic and Antarctic products	Heights of sea ice and open water samples (at TBD length scale) relative to ellipsoid after adjusted for geoidal and tidal variations, and inverted barometer effects. Includes surface roughness from height statistics and apparent reflectance	There will be files for each pole per orbit
08/ L3	Land Water Vegetation Heights	Uniform sampling along-track for each beam pair and variable footpath	Heights of ground including inland water and canopy surface at TBD length scales. Where data permits, include estimates of canopy height, relative canopy cover, canopy height distributions (decile bins), surface roughness, surface slope and aspect, and apparent reflectance. (Inland water > 50 m length -TBD)	Per half (TBD) orbit
09/ L3	ATLAS Atmosphere Cloud Layer Characteristics	Based on 3 profiles at a 25 Hz rate. (400 laser pulses are summed for each of the 3 strong beams.)	Cloud and other significant atmosphere layer heights, blowing snow, integrated backscatter, optical depth	Per day
10/ L3	Arctic Sea Ice Freeboard / Antarctic Sea Ice Freeboard	Along-track all beams. Freeboard estimate along-track (per pass); separate Arctic/ Antarctic products	Estimates of freeboard using sea ice heights and available sea surface heights within a ~TBD km length scale; contains statistics of sea surface samples used in the estimates.	There will be files for each polar region per day
11/ L3	Antarctica Ice Sheet H(t) Series/ Greenland Ice Sheet H(t) Series	Height time series for pre-specified points (every 200m) along-track and Crossovers.	Height time series at points on the ice sheet, calculated based on repeat tracks and/or crossovers	There will be files for each ice sheet for each year
12/ L3A	Ocean Height	Along-track heights per beam for ocean including coastal areas	Height of the surface 10 Hz/700 m (TBD) length scales. Where data permits, include estimates of height distributions (decile bins), surface roughness, surface slope, and apparent reflectance	Per half orbit
13/ L3	Inland Water Height	Along-track height per beam	Along-track inland ground and water height extracted from Land/Water/ Vegetation product. TBD data-derived surface indicator or mask. Includes	TBD files Per day

**ICESat-2 Algorithm Theoretical Basis Document for Gridded Dynamic Ocean Topography**

**Release 001**

			roughness, slope and aspect.	
--	--	--	------------------------------	--

<b>File ID/Level</b>	<b>Product Name</b>	<b>Concept</b>	<b>Short Description</b>	<b>Frequency</b>
14/L4	Antarctica Ice Sheet Gridded/ Greenland Ice Sheet Gridded	Height time series interpolated onto a regular grid for each ice sheet. Series (5-km posting interval)	Height maps of each ice sheet for each year of the mission, based on all available ICESat-2 data.	Per ice sheet per year
15/L4	Antarctica Ice Sheet dh/dt Gridded/ Greenland Ice Sheet dh/dt Gridded	Images of dh/dt for each ice sheet, gridded at 5 km.	Height-change maps of each ice sheet, with error maps, for each mission year and for the whole mission.	Per ice sheet for each year of mission, and for the mission as a whole
16/ L4	ATLAS Atmosphere Weekly	Computed statistics on weekly occurrences of polar cloud and blowing snow	Polar cloud fraction, blowing snow frequency, ground detection frequency	Per polar region Gridded 2 x 2 deg. weekly
17/ L4	ATLAS Atmosphere Monthly	Computed statistics on monthly occurrences of polar cloud and blowing snow	Global cloud fraction, blowing snow and ground detection frequency	Per polar region Gridded 1 x 1 deg. Monthly
18/L4	Land Height/ Canopy Height Gridded	Height model of the ground surface, estimated canopy heights and canopy cover gridded on an annual basis. Final high resolution DEM generated at end of mission	Gridded ground surface heights, canopy height and canopy cover estimates	Products released annually at a coarse resolution (e.g. 0.5 deg. tiles, TBD). End of mission high resolution (~1-2km)
19/ L4	Ocean MSS	Gridded monthly	Gridded ocean height product including coastal areas. TBD grid size. TBD merge with Sea Ice SSH	Monthly

**ICESat-2 Algorithm Theoretical Basis Document for Gridded Dynamic Ocean Topography**

**Release 001**

20/ L4	Arctic and Antarctic Gridded Sea Ice Freeboard/	Gridded monthly; separate Arctic and Antarctic products	Gridded sea ice freeboard. (TBD length scale)	Aggregate for entire month for each polar region
--------	---	---	---	--

<b>File ID/Level</b>	<b>Product Name</b>	<b>Concept</b>	<b>Short Description</b>	<b>Frequency</b>
21/ L4	Arctic Gridded Sea Surface Height within Sea Ice/ Antarctic Gridded Sea Surface Height within Sea Ice	Aggregate for entire month (all sea surface heights within a grid) separate Arctic and Antarctic products	Gridded monthly sea surface height inside the sea ice cover. TBD grid	Aggregate for entire month for each polar region
22/L4	Inland water daily product			
Experimental	Arctic Sea Ice Thickness / Antarctic Sea Ice Thickness	Per Pass Thickness samples (from 10-100m freeboard means) for every 10 km (TBD) segment (all beams) where leads are available; (per pass)	Sea ice thickness estimates derived from the sea ice freeboard product. External input: snow depth and density for each pass.	There will be files for each polar region per day
Experimental	Arctic Gridded monthly Sea Ice Thickness / Antarctic Gridded monthly Sea Ice Thickness	Aggregate for entire month (all thickness observations within a grid) plus Thickness (corrected for growth)	Gridded sea ice thickness product; centered at mid-month. Include thickness with or without adjustment for ice growth (based on time differences between freeboard observation).	Gridded monthly (all thickness observations within a grid) for each polar region



*ICESat-2 Algorithm Theoretical Basis Document for Gridded Dynamic Ocean Topography*

**Release 001**

Experimental	Lake Height	Along reference track per beam in Pan-Arctic basin (>50-60 deg N).	Extracted from Product 08 and 13, for lakes >10 km <sup>2</sup> , with slope and aspect. Ice on/off flag. TBD water mask developed from existing masks.	Monthly along track product, no pointing
Experimental	Snow Depth	Along reference track per beam for Pan-Arctic basin (>50-60 deg N).	Extracted from Product 08 and 13 along track repeat heights, with slope and aspect. Snow detection flag.	Monthly along track product, no pointing

## APPENDIX B: Fitting a Plane to Spatially Distributed Data

To evaluate the average DOT at the center of a grid cell we fit a plane to all the samples within the 8 grid cells surrounding the cell and evaluate the height of the plane at the center of the grid cell. To do this we first have to make a least-squares fit of a plane to DOT at  $N$  locations within the grid cell. Following *Eberly (2019)*, given data (DOT) as a function of  $x$  and  $y$ ,  $h_i = f(x_i, y_i)$  at  $i=1$  to  $N$  locations, find a least squares fit of a plane, coefficients  $a$ ,  $b$ ,

and  $c$ , to  $h_i$  with mean,  $\bar{h} = \left(\frac{1}{N}\right) \sum_{i=1}^N h_i$ . (Also note  $\bar{x} = \left(\frac{1}{N}\right) \sum_{i=1}^N x_i$  and  $\bar{y} = \left(\frac{1}{N}\right) \sum_{i=1}^N y_i$  )

$$h_i \approx ax_i + by_i + c \tag{1}$$

And we want to choose  $a$ ,  $b$ , and  $c$  such that the error,  $E$ ,

$$E(a,b,c) = \sum_{i=1}^N ((ax_i + by_i + c) - h_i)^2$$

is minimized. According to *Eberle (2019)* the solution is more robust and the equations are simpler if we initially eliminate the need to determine  $c$  by taking the average of (1) and subtracting it from (1), to get:

$$h_i - \bar{h} \approx a(x_i - \bar{x}) + b(y_i - \bar{y})$$

and so for the deviations  $h'_i = h_i - \bar{h}$  ,  $x'_i = x_i - \bar{x}$  , and  $y'_i = y_i - \bar{y}$   
 (2)

$$h'_i \approx ax'_i + by'_i \tag{3}$$

and we will choose  $a$  and  $b$  to minimize:

$$E(a,b) = \sum_{i=1}^N ((ax'_i + by'_i) - h'_i)^2 \tag{4}$$

Then  $c$  will be given by  $c = \bar{h} - (a\bar{x} + b\bar{y})$ . To minimize  $E$  with respect to  $a$  and  $b$  we find  $a$  and  $b$  for which:

$$\begin{aligned} \frac{\partial E(a,b)}{\partial a} &= 2 \sum_{i=1}^N x'_i ((ax'_i + by'_i) - h'_i) = 2 \sum_{i=1}^N ax'_i x'_i + bx'_i y'_i - x'_i h'_i = 0 \\ \frac{\partial E(a,b)}{\partial b} &= 2 \sum_{i=1}^N y'_i ((ax'_i + by'_i) - h'_i) = 2 \sum_{i=1}^N ay'_i x'_i + by'_i y'_i - y'_i h'_i = 0 \end{aligned}$$

or

$$a \sum_{i=1}^N x'_i x'_i + b \sum_{i=1}^N x'_i y'_i = \sum_{i=1}^N x'_i h'_i$$

$$a \sum_{i=1}^N y'_i x'_i + b \sum_{i=1}^N y'_i y'_i = \sum_{i=1}^N y'_i h'_i$$

Letting

$$L_{xx} = \sum_{i=1}^N x'_i x'_i \quad R_{xh} = \sum_{i=1}^N x'_i h'_i$$

$$L_{yy} = \sum_{i=1}^N y'_i y'_i \quad \text{and} \quad R_{yh} = \sum_{i=1}^N y'_i h'_i$$

$$L_{xy} = \sum_{i=1}^N y'_i x'_i$$
(5)

a, b, and c are given by

$$a = \frac{R_{xh}L_{yy} - R_{yh}L_{xy}}{L_{xx}L_{yy} - L_{xy}^2}$$

$$b = \frac{R_{yh}L_{xx} - R_{xh}L_{xy}}{L_{xx}L_{yy} - L_{xy}^2}$$

$$c = \bar{h} - (a\bar{x} + b\bar{y})$$
(6)

Eberle, D., 2019, Least Squares Fitting of Data by Linear or Quadratic Structures

David Eberly, Geometric Tools, Redmond WA 98052

<https://www.geometrictools.com/>

This work is licensed under the Creative Commons Attribution 4.0 International License.

To view a copy

of this license, visit <https://creativecommons.org/licenses/by/4.0/> or send a letter to

Creative Commons,

PO Box 1866, Mountain View, CA 94042, USA.

Created: July 15, 1999

Last Modified: February 14, 2019

<https://www.geometrictools.com/Documentation/LeastSquaresFitting.pdf>

## APPENDIX C: Hierarchy of ATL12 and ATL19 Variables

### ATL12 Inputs to ATL19

Segment Averages: *SSH- geoid\_seg, lat\_seg, lon\_seg, bin\_ssbias, geoid\_seg, depth\_ocn\_seg, length\_seg*, and *surf\_type\_prcnt*.

Segment Moments: *SSHvar, SSHskew, SSHkurt, swh*

Segment Histogram: *Y, n\_photons*

Segment Degrees-of-Freedom: *NP\_effect*

### 3.2.4.2.1 Output ATL19 Averaging Over *n segs* Bins

Grid Cell Averages: *dot\_avg, lat\_avg, lon\_avg, ssb\_avg, geoid\_avg, depth\_avg, surf\_avg*

Grid Cell Average Moments: *dot\_sigma\_avg, dot\_skew\_avg, dot\_kurt\_avg, swh\_avg*

Grid Cell Total Histogram: *dot\_hist*

Grid Cell Totals: *n\_segs, n\_phs\_ttl, n\_ph\_srfc, length\_sum*

Grid cell DOT Uncertainty: *dot\_avg\_uncrtn*

### 3.2.4.2.2 Output ATL19 Averaging Weighted by Degrees-of-Freedom

Grid Cell Degree-of-Freedom Weighted Averages *dot\_dfw, grid\_lat\_dfw, grid\_lon\_dfw, , ssb\_dfw, geoid\_dfw, depth\_dfw, length\_dfw, surf\_prcnt\_dfw*,

Grid Cell Degree-of-Freedom Weighted Moments *dot\_sigma\_dfw, dot\_skew\_dfw, dot\_kurt\_dfw, swh\_dfw*

Grid Cell Degrees-of-Freedom and DOT Uncertainty: *dof, dot\_dfw\_uncrtn*

### 3.2.4.3 Output ATL19 Merging All-Beam, variables

All single beam gridded variables have all-beam versions, except for gridded skewness and gridded kurtosis. The all-beam variable names end in ‘\_albm’.

### 3.2.4.4.1 Output ATL19 Interpolated to Bin Centers (*gridcntr lon* and *gridcntr lat*)

Averages at Grid Cell Center: *dot\_avgcntr avgcntr, depth\_avgcntr, geoid\_avgcntr, ssb\_avgcntr, swh\_avgcntr*

### 3.2.4.4.2 Output ATL19 Interpolated to Bin Centers (*gridcntr* and *gridcntr lat*)

DOF Weighted Averages at Grid Cell Center: *dot\_dfwcntr, depth\_dfwcntr, geoid\_dfwcntr, ssb\_dfwcntr, swh\_dfwcntr*

*ICESat-2 Algorithm Theoretical Basis Document for Gridded Dynamic Ocean Topography*  
**Release 001**

## APPENDIX D: All-beam Average Equivalencies

The all-beam parameters can be computed in the same way single beam averages are computed by merely incorporating all the ocean segments from all beams in a grid cell. However the results should be the same as the properly weighted single beam averages as described below

The photon all-beam (\**albm*) totals are computed first. For all-beam total surface reflected photons, *n\_ph\_srfcalbm* add the number of surface reflected photons, *n\_ph\_srfc*, for each beam, and for the all-beam total of all photons in the downlink bands, *n\_phs\_ttl\_albm*, add the grid cell totals, *n\_phs\_ttl*, for each beam. Further, the all-beam photon rate, *r\_srfc\_albm*, is equal to *n\_ph\_srfcalbm* divided by *length\_sum\_albm*, the total of the total length of segments, *length\_sum*, for each beam. Similarly, the all-beam noise rate, *r\_noise\_albm* equals (*n\_phs\_ttlalbm* minus *n\_ph\_srfcalbm*) divided by *length\_sum\_albm*.

### All-beam Average DOT

The average DOT of data from all six beams in the cell, *dot\_avg\_albm* should equal.

$$dot\_avg\_albm = \{ \text{Sum } [n\_segs * dot\_avg]_{\text{beams 1 to 6}} \} / \text{Sum } [n\_segs]_{\text{beams 1 to 6}}$$

The following variables have all-beam gridded simple averages that can be calculated in the same way: depth, geoid, lat, lon, ssb, surf\_prcnt and swh. The variable names all end in *\_avg\_albm*.

### All-beam Degree-of-Freedom Weighted Average DOT

The degree-of-freedom average DOT of all six beams in the cell, *dot\_dfw\_albm* should equal

$$dot\_dfwalbm =$$

$$(\text{Sum } [dof * dot\_dfwcntr]_{\text{beams 1 to 6}}) / \text{Sum } [dof]_{\text{beams 1 to 6}},$$

For each grid cell we also can compute the all-beam degrees of freedom *dof\_albm*, the all-beam degree-of-freedom weighted standard deviation, *dot\_sigma\_dfwalbm*, and DOT uncertainty, *dot\_dfw\_uncrtn\_albm*.

$$dof\_albm = \text{Sum } [dof]_{\text{beams 1 to 6}}$$

$$dot\_sigma\_dfwalbm = ((\text{Sum } [dof * (dot\_sigma\_dfw)^2]_{\text{beams 1 to 6}}) / dof\_albm)^{1/2}$$

$$dot\_dfw\_albm\_uncrtn = dot\_sigma\_dfwalbm / (dof\_albm)^{1/2}$$

*ICESat-2 Algorithm Theoretical Basis Document for Gridded Dynamic Ocean Topography*  
**Release 001**

## APPENDIX E: Optimal Interpolation of ICESat-2 Dynamic Ocean Topography

This section in anticipation of future ATL19 features is largely excerpted from Harry Stern’s optimal interpolation notes, “HSnote1998”, 7/2/1998 with additions from David Morison’s Kriging series: “Kriging7\_JM”, 2/23/2021.

### Optimal Interpolation

We want to estimate or interpolate a true field of surface height or dynamic ocean topography,  $H(x)$ , by an approximation  $\hat{H}$  of the form

$$\hat{H} = \sum_{j=1}^n a_j(x) \hat{H}_j \tag{E1}$$

In this expression:

$x$  is a spatial coordinate. We could just as well have written  $H(x,y,z)$  to estimate  $H$  in 3-D. The number of spatial dimensions makes no difference in the following development. The coordinate  $x$  or coordinates  $x, y, z$  are just parameters.

$\hat{H}_j$  are observations at spatial coordinate  $x_j$ .

$a_j(x)$  are unknown functions that we will determine. We could just as well have written  $a_j(x,y,z)$  for the 3-D case.

So the estimate  $\hat{H}(x)$  is a linear combination of the measurements  $\hat{H}_j$ . We will sometimes drop the reference to the spatial coordinate  $x$  and just write  $H$ ,  $\hat{H}$ , and  $a_j$  with the understanding that these depend on the spatial coordinates.

We suppose that each measurement,  $\hat{H}_j$ , consists of a true value  $H_j$  plus a measurement error  $\delta_j$ :

$$\hat{H}_j = H_j + \delta_j \tag{E2}$$

So  $H_j = H(x_j)$  is the true value of the field  $H(x)$  at the measurement point  $x_j$ .

Now we form the error expression between the true field and the estimate,  $\epsilon = H - \hat{H}$ , using (E1) and (E2). We write  $\epsilon^2$  as

$$\epsilon^2 = \left[ H - \sum_{j=1}^n a_j (H_j + \delta_j) \right]^2 \tag{E3}$$



At this point we introduce the idea of random variables. We consider the true value of  $H(x)$  to be an ensemble or collection of values, a random variable with some mean and variance. Similarly, the  $H_j$  are random variables. The measurement errors,  $\delta_j$ , are random variables with zero mean. The coefficients  $a_j$  are not random variables. We use the notation  $E[...]$  for the expected value of a random variable. We want to determine coefficients,  $a_j$ , by minimizing  $E[\varepsilon^2]$ . To minimize the error with respect to the  $a_j$ , we set the derivative of the error with respect to each coefficient equal to zero. Assuming the errors and true heights are uncorrelated, we find the  $n$  coefficients are given by a system of  $n$  equations for the  $n$  coefficients.

$$\sum_{j=1}^n \frac{E[H_j H_k]}{E[H^2]} a_j + \sum_{j=1}^n \frac{E[\delta_j \delta_k]}{E[H^2]} a_j = \frac{E[HH_k]}{E[H^2]} \quad (\text{E4})$$

The expression  $E[\delta_j \delta_k]$  is the covariance of the measurement errors. If we make the assumption that the errors are uncorrelated then this term is zero when  $j \neq k$ , and we write  $E[\delta_k^2] = \sigma_k^2$  for the variance of the  $k^{\text{th}}$  measurement error. Then the second term in (E4) reduces to  $\frac{\sigma_k^2}{E[H^2]} a_k$ .

Now we return to the idea of the background or mean field. The expressions

$$\frac{E[H_j H_k]}{E[H^2]} \quad \text{and} \quad \frac{E[HH_k]}{E[H^2]} \quad (\text{E5})$$

would be correlations if the mean of  $H$  were zero. Since we want to interpret them as correlations, we must insist that  $H$  have zero mean. Also  $E[H^2]$  is not a variance unless  $H$  has a zero mean. So we have to modify our thinking about  $H(x)$ . We are free to construct any background field,  $B(x)$ , that we like. And we may subtract  $B$  from  $H$  and  $\hat{H}$  to get the deviations from the background:

$$h = H - B \quad \text{and} \quad \hat{h} = \sum_{j=1}^n a_j \hat{h}_j \quad \text{where} \quad \hat{h}_j = \hat{H}_j - B(x_j)$$

We go through the derivation of (E4) with  $h$  and  $\hat{h}$  instead of  $H$  and  $\hat{H}$  and end up with terms corresponding to (E5):

$$\frac{E[h_j h_k]}{E[h^2]} \text{ and } \frac{E[hh_k]}{E[h^2]} \quad (\text{E6}),$$

which are correlations because  $h$  has zero mean. So whatever background field we construct, it must be a mean field in the sense that it leaves zero mean fluctuations when subtracted from  $H(x)$  (in which case  $E[h]$  equals zero and  $E[\varepsilon^2]$  equals the variance of  $\varepsilon$ ).

We now return to (E4) and consider  $h$  (and  $h_j$ ) to be fluctuations from the background field  $B(x)$  such that  $E[h]$  equals zero. Note that this requires subtracting  $B_j$  (equal to  $B(x_j)$ ) from the measurements  $\hat{H}_j$ :

$$\hat{h} = \sum_{j=1}^n a_j (\hat{H}_j - B_j) \quad (\text{E7})$$

and re-interpreting  $\hat{H}$  as well, i.e., adding  $B(x_j)$  to  $\hat{h}$  to obtain  $\hat{H}$ . With the assumption of uncorrelated measurement errors equation (E4) becomes:

$$\sum_{j=1}^n \frac{E[h_j h_k]}{E[h^2]} a_j + \frac{\sigma_k^2}{E[h^2]} a_k = \frac{E[hh_k]}{E[h^2]} \quad (\text{E8})$$

or

$$(\mathbf{R} + \mathbf{D})\bar{a} = \bar{s} \quad (\text{E9})$$

where we use the matrix notation to denote:

$\mathbf{R}$  = the correlation matrix of the fluctuation field between all pairs of locations where measurements are made. The  $(j,k)$  entry of this  $n \times n$  symmetric matrix is  $E[h_j h_k]$  over  $E[h^2]$ .

$\mathbf{D}$  = the diagonal matrix with entries  $\sigma_k^2 / E[h^2]$  giving the ratio of measurement error variance to field fluctuation variance.

$\bar{a}$  = the vector of unknown interpolation coefficients,  $a_k$ ,  $k = 1$  to  $n$ .

$\bar{s}$  = the vector of correlations between location  $x$  and location  $x_k$  ( $k=1$  to  $n$ ) with entries  $E[h h_k]$  over  $E[h^2]$ .

Equation (E9) is a system of  $n$  equations in  $n$  unknowns. Notice that the only dependence on location  $x$  is in the right-hand side  $\bar{s}$ .

### **Kriging as a form of Optimal Interpolation**

Note that (E9) is very similar to D. Morison's "Kriging\_7" equation (12) for simple Kriging:

$$0 = -[z\mathbf{Z}_j] + [\mathbf{Z}_j\mathbf{Z}_i] \mathbf{w}_i \quad (\text{DM12})$$

or

$$\mathbf{R}_K \bar{\mathbf{a}} = \bar{\mathbf{s}}_K \quad (\text{DM12b})$$

where  $\mathbf{R}_K = [\mathbf{Z}_j\mathbf{Z}_i]$  is the covariance matrix of observations,  $\bar{\mathbf{a}} = \mathbf{w}_i$  is the vector of weights, and  $\bar{\mathbf{s}}_K = [z\mathbf{Z}_j]$  is the vector of covariances between heights at location  $x$  and locations  $x_j$ .

The Kriging equation (DM12) is similar to (E4) and the vector of weights would be the same, but the covariances are not normalized by the variance of the heights  $E[h^2]$ , i.e.,  $\mathbf{R}_K = \mathbf{R}E[h^2]$  and  $\bar{\mathbf{s}}_K = \bar{\mathbf{s}}E[h^2]$ . Perhaps more importantly for our application, Kriging makes no *a priori* distinction as to measurement noise so that in Kriging, variability due to measurement noise and the natural variability of the measured variable are mixed together at the measurement locations; essentially,  $\mathbf{R}_K = \mathbf{R} + \mathbf{D}$  of equation (E9).

With ICESat-2 ATL12 SSH and ATL19 gridded DOT data we have calculated uncertainties, which are essentially the measurement errors for the mean SSH in ATL12 ocean segments and grid-cell averages of DOT in ATL19. Therefore, in principle, we can take advantage of Equation (E4) because we have a formalism for distinguishing between measurement noise,  $\mathbf{D}$ , and process variability,  $\mathbf{R}$ , in the analysis.

### **Elements Needed for Optimal Interpolation of ICESat-2**

To summarize, what do we need to get the coefficients to use (E1) to optimally interpolate data? We need (1) a background or prior estimate of the height,  $\mathbf{B}$ , as a function of the dimensional variable or variables,  $x$  or  $x, y, z$ , (2) a square correlation matrix of the observations,  $\mathbf{R}$ , (3) a diagonal matrix of measurement errors or uncertainties,  $\mathbf{D}$ , and (4) a  $n \times 1$  vector of correlations between the interpolant points and the observation points,  $\bar{\mathbf{s}}$ .

Background,  $\mathbf{B}$  – The background field,  $\mathbf{B}$ , can in principle be anything that has a mean equal to the mean of the observations. However, if the mean of the observations is used for the background, all of the variability even out to the largest scales will be included in the correlation matrix,  $\mathbf{R}$ . This is unrealistic when the data domain is the global ocean, especially when we want to interpolate over a short distance, e.g., 25 km, and the physical process we want to examine has a correlation length constrained by physics. For example, the DOT measured in the Southern Ocean has nothing to do with interpolating to a 25 km grid off the coast of Greenland. In this case it makes sense to choose as a background field a climatology averaged over larger space and time scales, for which simple averaging can be done with minimal interpolation. The pertinent example is the 9-cell, 3-month averages of ICESat-2 DOT to cell centers (e.g., Figure 6, right). These can be done monthly and for

almost every grid cell. And the 91-day repeat cycle of ICESat-2 is such that the 9-cell, 3-month averages have the potential for at least one satellite pass over every grid cell, so only cells under virtually perpetual cloud cover will need to have background values interpolated to them. At least initially this can be done with simple linear interpolation, and then be iterated with near optimal interpolation coefficients from prior iterations.

Correlation Matrix,  $\mathbf{R}$  –  $\mathbf{R}$  is the covariance or correlation (the difference being the correlation matrix is covariance matrix divided by the variance) for the true data. Because we don't actually know the true data anywhere but in particular at the point to which we want to interpolate, we have to have a model of the covariance matrix based on the covariance of observations. These can be the observations that we want to interpolate or observations in the same or similar locations made in the past. In solving equation (E4) we can use the  $\mathbf{R}$  of the actual observations to be interpolated. However, we don't have that luxury for covariances between the data points and the points with no data,  $\bar{s}$ . To make it generally applicable, the covariance matrix rests on a data-based model of the correlation of the variable as a function of separation in the relevant dimensions over which it is being interpolated, for example a Gaussian or decaying exponential with separation distance.

Following Kriging7\_JM, we can derive the covariance model using the observed covariogram  $E[h_j h_k]$  and  $E[hh_k]$  (or  $[\mathbf{Z}_j \mathbf{Z}_i]$  and  $[z \mathbf{Z}_i]$  in the parlance of Kriging7\_JM). These are assumed to be dependent on only the separation between observation points and are therefore represented by a model of the covariogram equal to  $E[h_j h_k]$  evaluated as a function of the distance,  $d_{jk}$ , separating observation locations  $j$  and  $k$ :

$$\mathbf{C}_{jk}(d_{jk}) = E[h_j h_k] \quad (\text{E10})$$

where  $\mathbf{C}_{jk}(d_{jk})$  is the covariogram of the observations sorted by distance between observation locations.

Although  $E[h_j h_k]$  and  $E[hh_k]$  are in principle covariances of the true height values, the covariogram models are based on the observations at the observed locations. If we have a data set with the same spatial statistics as the variable we are interested in interpolating, or if there are sufficiently representative observations in the data set of interest, we can construct a sample covariogram. For every possible pair of values in the sample data, we calculate the product of the values of each sample pair as a function of the distance between each sample pair. For example from the column vector of observation,  $\vec{h}$ , we can form the symmetric covariance matrix,  $\mathbf{C}_H$ :

$$\mathbf{C}_{jk} = \vec{h} \vec{h}' = \begin{pmatrix} c_{11} & \cdots & c_{1n} \\ \vdots & \ddots & \vdots \\ c_{n1} & \cdots & c_{nn} \end{pmatrix} \quad (\text{E11})$$

We also form the symmetric matrix of separation distances  $D_{jk}$  :

$$D_{jk} = \begin{pmatrix} d_{11} & \cdots & d_{1n} \\ \vdots & \ddots & \vdots \\ d_{n1} & \cdots & d_{nn} \end{pmatrix} \quad (E12)$$

where  $d_{jk}$  equals the distance between observation points  $j$  and  $k$ . We then take all the values,  $c_{jk}$ , in the upper right half and diagonal of  $C_{jk}$  paired with the corresponding  $d_{jk}$ , and order them in ascending values of  $d_{jk}$ . The resulting array of covariance values versus separation distance can be fit with a functional model of correlation versus distance. The most common forms are decaying exponentials or Gaussians.

$$C_V(d) = C_{oeff} e^{(-d/L)} \quad (E13)$$

or

$$C_V(d) = C_{oeff} e^{(-0.5(d/L)^2)} \quad (E14)$$

with correlation length scale,  $L$ , and coefficient,  $C_{oeff}$ , to be adjusted to fit the covariance versus separation distance data.

Note that if we thought the correlations were different for separations in two different directions we could fit  $C_{jk}(d_{xjk}, d_{yjk}) = [h_j h_k]$  as a function of  $d_x$  and  $d_y$  to get a model  $s_x$  and  $s_y$  and covariogram  $V(d_x \text{ and } d_y)$ , exponential:

$$C_V(d_x, d_y) = C_{oeff} e^{-k_x d_x} e^{-k_y d_y} \quad (E15)$$

or Gaussian:

$$C_V(d_x, d_y) = C_{oeff} e^{(-0.5(d_x/s_x)^2)} e^{(-0.5(d_y/s_y)^2)} \quad (E15)$$

Interpolant Correlation Vector,  $\vec{S}$  - The vector  $\vec{S}$  is the vector of correlations between location  $x$  and location  $x_k$  ( $k=1$  to  $n$ ) with entries  $E[h h_k]$  over  $E[h^2]$ . In this case we absolutely have to have the model of covariance, because by definition there are no data for  $h$  at the interpolant point. For example, using an exponential model of the covariogram for  $\vec{S}$  we set

$$C_j(d_j) = E[h h_j] = C_{oeff} e^{(-d_j/L)} \quad (E16)$$

where  $C_j(d_j)$  is the model covariogram as a function of the distance,  $d_j$ , between the observation locations and the location of the point to be interpolated. Note that if the constellation of measurement points was changed, for example made smaller to interpolate closer to a coastline, the same modeled correlation function from the original covariogram could be used with a smaller subset of the original observation points to form  $\mathbf{R}$ .

Measurement Error Matrix  $\mathbf{D}$  – The matrix  $\mathbf{D}$  is the diagonal matrix with entries  $\sigma_k^2/E[h^2]$ . Because the correlation of the true  $h(x)$  with itself is 1, the diagonal elements of  $\mathbf{R}_K = \mathbf{R} + \mathbf{D}$  are going to be equal to the natural variance of  $h$  as a function of location plus the measurement variance. When we use the covariogram of observations to model  $\mathbf{R}_K$ , the diagonal elements will devolve into a constant that includes natural variability and the variance due to measurement noise. Our known uncertainties from ATL12 will not enter into determining the optimal interpolation coefficients for the surface height anomalies about the background. However, we can examine the fit of the covariogram for small separation distances and extrapolate to zero separation. This will give an estimate of the average of the natural or true variance at zero separation, i.e., the diagonal elements of  $\mathbf{R}$ . The difference between the covariance extrapolation to zero separation and the observed covariance at zero separation should be similar to the uncertainties from ATL12. If it is not, we may choose to adjust the fit to the covariogram data by subtracting the average measurement noise from the covariogram data at zero separation. The resulting model  $\mathbf{R}$  can be compared with the covariances estimated from ocean models and other observations.